ASSESSMENT OF RENEWABLE ENERGY BASED MICRO-GRIDS FOR SMALL COMMUNITIES

SUSTAINABLE ENVIRONMENT AND ENERGY SYSTEMS

MIDDLE EAST TECHNICAL UNIVERSITY

NORTHERN CYPRUS CAMPUS

BY

S.M.SAJED SADATI

IN PARTIAL FULFILLMENT OF THE REQUIREMENTS

FOR

THE DEGREE OF MASTER OF SCIENCE

IN

SUSTAINABLE ENVIRONMENT AND ENERGY SYSTEMS PROGRAM

JULY 2016

Approval of the Board of Graduate Programs

____

Prof. Dr. M. Tanju Mehmetoğlu
Chairperson

I certify that this thesis satisfies all the requirements as a thesis for the degree of Master of Science

Assoc. Prof. Dr. Ali Muhtaroğlu
Program Coordinator

This is to certify that we have read this thesis and that in our opinion it is fully adequate, in scope and quality, as a thesis for the degree of Master of Science.

Asst. Prof. Dr. Onur Taylan
Supervisor

Examining Committee Members

Assoc. Prof. Dr. Murat Fahrioğlu	Electrical and Electronics Engineering, METU NCC	
Asst. Prof. Dr. Onur Taylan	Mechanical Engineering, METU NCC	
Prof. Dr. Derek K. Baker	Mechanical Engineering, METU	

I hereby declare that all information in this document has been obtained and presented in accordance with academic rules and ethical conduct. I also declare that, as required by these rules and conduct, I have fully cited and referenced all material and results that are not original to this work.

Name, Last Name: S.M.Sajed Sadati

Signature:

ABSTRACT

ASSESSMENT OF RENEWABLE ENERGY BASED
MICRO-GRIDS FOR SMALL COMMUNITIES

Sadati, S.M.Sajed

M.Sc., Sustainable Environment and Energy Systems

Supervisor: Asst. Prof. Dr. Onur Taylan

July 2016, 84 pages

Deploying renewable energy systems to supply electricity faces many challenges related to cost and variability of the renewable resources. One possible solution to these challenges is to hybridize renewable energy systems with conventional power systems and include energy storage systems. In this study, the feasibility analysis of two cases for electricity generation systems as (*i*) photovoltaic (PV)-battery-pumped hydro system (PHS) and (*ii*) PV-wind-battery are presented as a Renewable Energy Micro-Grid (REMG) for a university campus-scale community on a Mediterranean island. The island has an isolated grid which generally utilizes fuel-oil based steam and diesel electric generators. Models for PV, wind turbine, battery and PHS systems are presented to estimate energy production, and net present cost (NPC) and levelized cost of electricity (LCOE) as economic metrics in the feasibility analysis. As a case study, Middle East Technical University Northern Cyprus Campus (METU NCC) with an average power demand of about 1 MW is considered. A parametric study is performed using a newly developed model for combining short-term and long-term energy storage systems integrated with PV systems for case (*i*) and HOMER software for case (*ii*) to determine the sizes of the components for the REMG. Both models are using hourly time-steps. In case (*i*), battery and PHS are considered as short- and long-term storage systems. For the studied ranges and considering the availability of water resources required for PHS, the lowest NPC of 40.65M USD is found for a configuration with 2.7 MW PV, 0.3 MWh battery and 2.5 MWh PHS. In case (*ii*), among all the configurations, two alternate configurations are proposed, one with storage and one without storage. Both configurations have identical NPCs of 38.3M USD, renewable energy fractions of 38% and 36%, respectively, and avoid approximately 4000 tons of CO_2 emissions per year. The system without storage consists of a 2 MW PV plant and 3 MW wind power system, and the system with storage consists of a 2 MW PV system, 3.75 MW wind power system and a 1 MWh battery. In both cases, the resulting LCOE is approximately 0.15 USD/kWh whilst the electricity tariff for METU NCC is approximately 0.175 USD/kWh.

Keywords: Renewable energy micro-grid, photovoltaic solar energy systems, wind energy, energy storage, economic assessment, Mediterranean island.

ÖZ

KÜÇÜK TOPLULUKLAR İÇİN YENİLENEBİLİR ENERJİ TEMELLİ MİKRO-ŞEBEKE DEĞERLENDİRMESİ

Sadati, S.M.Sajed

Yüksek Lisans, Sürdürülebilir Çevre ve Enerji Sistemleri

Tez Yöneticisi: Yrd. Doç. Dr. Onur Taylan

Temmuz 2016, 84 sayfa

Elektrik sağlamak için kurulan yenilenebilir enerji sistemleri, maliyet ve yenilenebilir enerji kaynaklarının değişkenlik göstermesi ile ilgili birçok zorlukla karşılaşmaktadırlar. Bu zorluklara karşı çözümlerden biri ise geleneksel elektrik üretim sistemlerini yenilenebilir enerji üretim sistemleri ile harmanlamak ve enerji depolama sistemlerini eklemektir. Bu çalışmada Akdeniz'deki bir adada bulunan kampüs ölçeğindeki bir topluluk için yenilenebilir enerji içeren mikro-şebeke olarak iki farklı elektrik üretme sisteminin fizibilite çalışması yapılmıştır. Bu iki sistem şu şekildedir: (*i*) fotovoltaik-akü/pil-pompajlı su depolama sistemi ve (*ii*) fotovoltaik-rüzgâr türbini-akü/pil. Örnek incelenen ada, anakaraya bağlantısı olmayan bir şebekeye sahiptir ve fuel oil yakan buhar ve dizel santralleri ile şebekeye elektrik sağlamaktadır. Bu çalışmada fotovoltaik güneş enerjisi sistemi, rüzgâr türbini, akü/pil ve pompajlı su depolama sistemine ait modeller; enerji üretimini, net bugünkü maliyeti (NPC) ve seviyelendirilmiş elektrik maliyetini (LCOE) tahmin etmek için verilmiştir. Örnek çalışma olarak, anlık ortalama elektrik tüketimi yaklaşık 1 MW olan Orta Doğu Teknik Üniversitesi Kuzey Kıbrıs Kampusu (ODTÜ KKK) ele alınmıştır. Sistem (*i*) için yeni geliştirilmiş model ile fotovoltaik sistemleri ile bütünleşik kısa ve uzun vadeli depolama sistemlerinin ve Sistem (*ii*) için HOMER yazılımı ile yenilenebilir enerji içeren mikro-şebekenin bileşenlerinin boyutlandırması parametrik çalışma olarak yapılmıştır. Bütün modellerde saatlik veriler kullanılmıştır. Sistem (*i*) bileşenlerinden akü/pil kısa vadeli ve pompajlı su depolama sistemi ise uzun vadeli depolama sistemleri olarak ele alınmıştır. Çalışılan parametre aralığı için ve pompajlı su depolama sistemi için gerekli su kaynaklarını düşünülerek elde edilen sonuçlara göre en düşük NPC 40,65 milyon USD ile 2,7 MW'lık fotovoltaik sistemi, 0,3 MWh'lık akü/pil ve 2,5 MWh'lik pompajlı su depolama sisteminden oluşan tasarıma ait çıkmıştır. Sistem (*ii*) için incelenen bütün tasarımlar arasında iki alternatif sistem önerilmektedir. Bu sistemlerden birisinde depolama sistemi mevcuttur, diğerinde ise depolama sistemi yoktur. Her iki alternatifin de NPC değerleri yaklaşık 38,3 milyon USD olup üretilen enerjide yenilenebilir enerji oranı %36 ile %38 aralığındadır. Ayrıca bu alternatiflerin yıllık yaklaşık 4000 ton CO_2 salınımı önlemesi öngörülmektedir. Depolama sistemi olmayan alternatif, 2 MW'lık fotovoltaik sistemi ile 3 MW'lık rüzgâr türbinlerinden oluşmaktadır. Depolama sistemi olan alternatif ise 2 MW'lık fotovoltaik sistemi, 3,75 MW'lık rüzgâr türbinleri ile 1 MWh'lik akü/pil depolama sisteminden oluşmaktadır. ODTÜ KKK için elektrik tarifesi yaklaşık 0,175 USD/kWh olup her iki alternatifin LCOE değeri 0,15 USD/kWh civarındadır.

Anahtar Kelimeler: Yenilenebilir enerji, mikro-şebeke, fotovoltaik güneş enerjisi sistemleri, rüzgar enerjisi, enerji depolama, ekonomik değerlendirme, Akdeniz adası.

DEDICATION

To *Elham* for her continuous supports.

ACKNOWLEDGEMENTS

I would like to thank my advisor, Dr. Onur Taylan for his kind supports throughout my studies at METU NCC. I would also like to thank Professor Derek Baker who initiated this work while I was taking a course on Renewable Energy Technologies with him. He provided me with the data on solar and wind energy and the software HOMER that I used for this study. Working with Dr. Taylan and Prof. Baker was a valuable experience for me. Similarly, I should thank Dr. Murat Fahrioglu and Kib-Tek for the data they provided on the electricity consumption at METU NCC.

I would also like to thank my parents, MirGhadir and Saeideh, who have always been supportive to me throughout my life and I believe that I owe many of the opportunities that I have had to their guidance.

I have learnt a lot about life and our journey as human beings from Afsaneh and Kourosh Salimi. They are the greatest masters that I have had the opportunity to meet. I am sincerely thankful of their effective and admirable efforts to spread joy, love and peace in the world.

I would like to thank Mechanical Engineering Program and METU NCC administration for offering me the teaching assistantship position which provided me with the financial supports and enabled me to pursue master studies at METU NCC. Moreover, I had the opportunity to have a part-time job at METU NCC library and I met the kindest people, Ms. Zuhal Topaloglu, Mr. Emir Sagdic, Mr. Cem Demirsoy, Mr. Fatih Sener and Ms. Mertcan Ceki. I had great times with them and I wish them happiness throughout their life.

Moslem Yousefzedeh and Maryam Kia introduced SEES program to me for the first time. The directions from them made it much easier for me to start and continue my studies as a SEES student.

I would also like to thank my greatest friends with whom I had lots of fun and memorable moments, Tahir, Hani, Parastoo, Zeynab, Alma, Hamed, Narges, Shahab, Tamanna, Reza, Melina, Mahdi, Negar, Mohammad, Gozde, Hasan Ali, Arsalan, Jibran, Abdullah, Fahad, Bushra, Fassahat, Sundas, Obaidullah, Madina, Humayun, Monazzah, Ali Hamza, Salih, Mr. Abdullah Onal, Kaya, Hamza and respected Rajabi Family.

My biggest thanks, however, goes to my wife, Elham, for her attitude and encouragement which has always been inspiring for me.

TABLE OF CONTENTS

LIST OF FIGURES

LIST OF TABLES

CHAPTER 1 – INTRODUCTION

Renewable energy systems (RES) are considered as the main alternatives for fossil fuel-based conventional power plants for generating electricity. The need for sustainable energy has been investigated in a large number of studies, e.g., [1]–[6]. The limited sources of energy and the environmental impacts of conventional thermal power plants are the main issues that make them unsustainable and undesirable in terms of being friendly to the environment [5], [6], while RES are advantageous from both aspects of availability and negligibility of their emissions. As reported by World Bank, in 2012 the electrical energy generation all over the world was about 26,783 TWh, including about 40.4% from coal, 22.4% from natural gas, 11.0% from nuclear, 16.1% from hydro, 4.1% from oil and 4.7% from renewable sources [7]. The renewable sources for generating electricity are mainly listed as solar (thermal and PV power plants), wind, geothermal, biofuels and waste usage [2], [5]. The total amount of the electricity generated by RES has been in a growing trend for last two decades, and global use of the renewable sources for generating electricity in 2005 was about 2% which was increased to 4.7% in 2012 [7]. This is still a very small share of the global electricity production. Therefore, it is required to study on ways and means for higher share of RES in the global electricity production. To this end, one promising way would be enabling RES-based micro-grids (REMG) which can be integrated with local conventional energy generation units which are termed as *hybrid* REMGs in this study.

Evans et al. [5] have introduced the two main challenges for deploying RES in large scales as higher specific cost of electricity produced by RES compared to electricity produced by conventional systems, and the variability of the renewable energy resources. These two challenges lead decision makers to consider hybrid systems as combinations of conventional energy technologies with RES to increase the RES share in the energy generation mix. Moreover, due to the variable nature of many renewable resources, considering a mix of different types of RES as a hybrid system along with deploying storage systems can increase the feasibility for higher RES share. Such a hybrid system could be capable of meeting the demand for 24 hours per day, 7 days per week (24/7) and be part of a micro-grid [8]. For conciseness and clarity, a Renewable Energy Micro-Grid (REMG) is defined herein as a micro-grid with one or more local renewable energy sources and which may or may not have storage. A differentiation is made between standalone and grid-connected REMGs, where grid-connected REMGs can island (disconnect) from the main grid and therefore operate as a standalone REMG for a considerable fraction of time in a year. A qualifier *hybrid* is used if the REMG is hybridized with local fossil-fuel based generation; e.g., standalone REMG versus standalone hybrid REMG. Currently aiming to achieve 24/7 electricity supply from a standalone REMG is generally expensive and in many cases should be considered as a long-term goal. In contrast, aiming to achieve 24/7 electricity supply through a grid-connected or standalone hybrid REMG is generally more economically feasible and can be considered as a short term goal. For grid-connected REMG, maximizing the islanding time fraction while preserving the feasibility of a grid-connected REMG is the goal of many REMG design studies. The feasibility for using REMG is often higher for communities with large local renewable resources such as solar and wind and characterized by nonexistent or unreliable, expensive, and/or dirty electricity supplies, which are termed isolated communities herein with respect to electricity supplies. Isolated communities are often found on islands, in rural areas, and in many urban areas in undeveloped or developing regions. Globally, there are still about 1.5 billion people living in isolated communities with no proper access to electricity, and often these areas have large renewable energy resources [9]–[12]. The electricity demand for these areas is commonly supplied by diesel generators which result in large uncertainties for fuel cost and externalize high pollution to the environment [9]. Therefore, REMG can be particularly appropriate for isolated communities, but there is still a need for further technology development and feasibility studies in this area.

Although implementing the REMGs is highly desired as alternatives for conventional power plants, there are still challenges arising from both technical and economic aspects due to the variability of renewable sources. For instance, solar energy is only available during day times with clear skies, and wind energy can be utilized whenever wind blows within a certain speed range. Hence, the main challenge in employing RES for generating electricity is the dispatchability of these systems. One way to resolve the problem of dispatchability is to store energy whenever available and use while demanded from energy storage systems (ESS).

1.1 Objective of the Study

There are three main objectives for this study. The first objective of this study is to build upon the available literature and integrate stationary ESS into REMG for small communities to utilize the unavoidable excess electricity and study the changes in RES fraction and the net present cost (NPC) of the REMG. The REMG consists of a PV system and two possible ESS types as short- and long-term storage systems for covering the hourly and seasonal energy needs which is connected to a local grid that runs by fossil fuel. These short- and long-term ESS types are considered to increase the RES fraction while decreasing the dependency on the local fossil fuel generators to meet the entire demand. NPC, LCOE and RES fraction are determined for different capacities of REMG's components in order to compare their performances. The methodology given in this study can be applied to any micro-grid, and herein as a case study for small communities which have limited/no access to stable electricity grids, it is applied to Middle East Technical University Northern Cyprus Campus (METU NCC) which is a university campus located on an island with no grid connection to a mainland. For the case study, an economic assessment of the currently installed PV system is conducted, and the effects of adding short- and long-term ESS on NPC, LCOE and RES fraction are analyzed and discussed.

The second objective is to design a RES that enables a grid-connected micro-grid which can be considered as a REMG for METU NCC using statistically-generated, synthetic typical meteorological year data that represent weather conditions expected over the long term. This is implemented by contrasting the feasibility of alternate REMGs for METU NCC using one or more of PV system, wind turbines and batteries, with the results potentially being important for any REMG in a Mediterranean climate, especially those for isolated communities.

The third objective is to evaluate the predicted performance of the designed REMG for METU NCC based on the measured solar and wind resources and sensitivity of the performance to the uncertainties in these resources. The results associated with the effect of the resources on the system's performance are potentially important for REMGs located anywhere.

1.2 Organization of This Work

Chapter 2 consists of a literature review to identify and assess the studies on the design of REMGs with and without ESS. The literature review is conducted on studies on deploying REMGs and studies related to applications of ESS for renewable energies. In Chapter 3, general energetic and economic models to design a REMG are given and the method to find the REMG with minimum NPC among the suggested capacities is described. In Chapter 4, the characteristics of and inputs for the METU NCC REMG case study are presented, including alternate hourly solar and wind resource models. While these characteristics and inputs are unique to METU NCC, the methodology used to develop these models can be adapted to other communities based on their unique characteristics. Chapter 5 includes the results of the analyses for NPC and LCOE versus PV system size and ESS capacity and the two design configurations suggested by HOMER that are considered to be the most feasible. The results are presented and discussed, including the analyses on their predicted performance using measured solar and wind data and its sensitivity to the availability of resources by varying them proportionally. In Section 5, conclusions and future work are presented. It should be noted that the parts of this work which are on the assessment of feasibility of a hybrid REMG consisting the three components of PV, wind and battery are adapted from the study by Sadati, Jahani, Taylan and Baker [23]. Specifically, this includes Sections 2.2, 4.2, and 5.3.

CHAPTER 2 – LITERATURE REVIEW

In this chapter, the current state of knowledge on deploying hybrid REMGs is reviewed in two subsections. The first subsection focuses on ESS for higher penetration of renewables in REMGs. The second one includes the studies for establishing REMGs with different RES configurations, specifically PV-wind-battery and fossil fuel based generators.

2.1 Energy Storage Systems for Renewable Energy Systems

There are several types of commonly used energy storage technologies which can be utilized in different sizes, from residential to grid scale applications. These technologies mainly include: (i) Thermal Energy Storage (TES); storing the thermal energy as latent or sensible heat in the materials, (ii) Compressed Air Energy Storage (CAES); compressing air in underground reservoirs, (iii) Pumped Hydro System (PHS); pumping water to a higher reservoir from a lower one and store the gravitational potential energy, (iv) Electrochemical Energy Storage; storing energy through chemical reactions which includes all types of batteries and fuel cells, and (v) Flywheels; storing the energy as mechanical kinetic energy [20]. Among these ESS types, TES, PHS and CAES are only suitable for large utility scale applications and long-term energy storage since the cost per unit energy capacity for those systems would be very high if they are installed with small capacities and the delay in charge and discharge processes would limit the energy utilization [18], [20], [21]. TES is suitable for energy generation technologies which mainly use heat engines like conventional fossil fuel based systems and solar thermal electric technologies [20], [26], [27]. In addition, CAES can only be used for gas turbine power plants to boost the energy production while less natural gas is consumed [20]. PHS is flexible for being installed with any energy generation technology as long as the required water and lower/upper reservoirs are available at the site of interest. The batteries have short response times and are more likely to be used in the case of small scale energy storage for residential buildings and micro-grids, mainly because they are more scalable comparing to other ESS types [21], [28]. Flywheels also have short response times and are more appropriate for stabilizing the electricity generation according to the frequency regulations when switching between the components of the REMG [18], [29]. In this study, which focuses on possibilities of ESS for PV systems for small communities, Zinc-Bromine batteries (ZBB) [30] and PHS are considered as possible short- and long-term storage systems. ZBB has lower capital cost comparing to the similar batteries with almost the same characteristics [29], and PHS is the only long-term ESS that can be integrated in large scales with a PV system [29]. It should be noted that to run the PHS a delay of 4 minutes should be considered [31] and the short-term ESS should be sized in a way that is able to cover the energy need of the system for this delay time. In other words, a minimum size of the short-term ESS which has a very short response time should be considered in the design of the system.

There are several studies on utilizing ESS to increase the penetration of renewable energy in the electricity distribution grids. For instance, Denholm and Hand [8] performed numerical analyses for flexibility of large grids and penetration of renewable energy sources like wind and solar in a large-scale electricity generation grid. They stated that renewable energy could be further utilized using a storage system, since it would enable RES to meet constant minimum load which is generally met by conventional thermal energy systems in a grid. Additionally, Kaldellis *et al.* [9] studied the application of ESS for REMGs in small islands and optimum selection of the type and size of the ESS. The objective was to meet the demand with the lowest cost of electricity using solar energy. Monthly average values for the insolation were used by Kaldellis et al. [9] and a constant annual demand and peak load were assumed to calculate minimum levelized cost of electricity (LCOE) for different types of ESS, considering a range of installed capacities for the PV system. In addition, Harris *et al.* [10] investigated the possible scenarios for using ESS in order to increase the possibility of having higher penetration of RES in the grid energy mix for Texas, USA. They stated that [10], optimal sizing of storage system requires higher time resolution data of insolation and demand. In addition, there are several other studies emphasizing the role of storage systems in the future of renewable energy technologies [11]–[15]. Moreover, Carbajales-Dale *et al.* [16] studied the ability of each renewable energy technology to support ESS. They used the capacity factor of each technology and the depth of discharge (DoD) which determines the maximum allowed level of discharge for the ESS as inputs to their models. They divided ESSs into two main groups: (i) geological storage, including compressed air and pumped hydro storage; and (ii) all types of batteries. Their results showed that higher installed capacities of geological ESS are technically and economically feasible for RES comparing with the feasible installed capacities of batteries. There are several other studies emphasizing the role of storage systems in the future of renewable energy technologies [11]–[15]. Moreover, several studies have been conducted on the characteristics and appropriate selection of the ESS type for the REMGs based on the availability and demand of the community for which the system was designed (e.g., [17]–[23]) while some have focused on the detailed modelling of specific ESS types (e.g., [24], [25]). Although the mentioned studies have focused on ESS applications, there is still a need for studies considering various options of stationary energy storage systems and their combinations integrated with the energy mix for finding the feasible ESS type and capacity with a focus on reducing the cost of the REMG. Implementing ESS for these cases would also increase the RES fraction which is defined here as the fraction of the electricity demand covered by RES. For an REMG, as the fraction of installed capacity for RES in the energy mix increases, the amount of the dumped energy, which is the excess electricity generated by RES that cannot be utilized/stored or sold to other communities, would also increase [8]. This dumped energy is an economical barrier for moving towards higher RES fractions, and implementing ESS would reduce the amount of the dumped energy significantly.

2.2 Hybrid REMGs

There are many studies in the recent literature on the feasibility of deploying REMGs for specific isolated communities to partially or entirely meet the demand, e.g., [9]–[12], [17], [37]–[43]. In all these studies, Levelized Cost of Electricity (LCOE) and RES fraction are reported as two important metrics for evaluating the performance of the system. Since designing a REMG requires the analysis of different parameters regarding availability of resources for a variety of components and technologies and the consideration of different possible sizes for each component, arriving at an optimal design can be difficult. To make this process easier, in some of these studies [9], [11], [39]–[43], HOMER software[1][44] was used. HOMER is an optimization tool for evaluating the design of different micro-grids, including REMG, with respect to minimizing the electricity cost or the fuel consumption. Using HOMER facilitates the evaluation of many possible system configurations and comparing them based on their NPC, LCOE and RES fractions. For instance, Bekele and Palm [41] studied the feasibility of a standalone solar and wind REMG for a rural area in

[1] Hybrid Optimization Model developed by National Renewable Energy Laboratory (NREL)

Ethiopia. Solar and wind resources for this study were estimated using models and satellite data as the inputs for HOMER. LCOE was reported for the REMG with different sizes to compare the economic feasibility of the systems. For instance, the reported LCOE were 0.383 and 0.464 USD/kWh for 51% and 81% RES fractions, respectively. Subsequently, Bekele and Tedesse [42] performed a similar study for Ethiopia for different standalone REMG designs including one or more of hydro, PV, wind, diesel generators and batteries. The LCOE ranged from 0.10 to 0.16 USD/kWh for RES fractions between 72% and 100%. Among all available choices the one with 95% RES fraction and LCOE of 0.108 USD/kWh was proposed as the best combination for maximizing the RES fraction with the lowest LCOE [42]. As another example, Giannoulis and Haralambopoulos [11] analyzed hybrid REMG options for Lesvos Island, Greece, using HOMER. In 2011 the infrastructure for electricity production in Lesvos consisted of two wind farms and one diesel power plant. Using the measured hourly wind data at the height of 33 m as the inputs for HOMER, the difference in the generated electrical energy estimated using HOMER and actually measured was about 1%. Moreover, Askari and Ameri [40] used HOMER to study the feasibility of different combinations of standalone REMG with battery storage for supplying the load requirements of a remote rural location in Kerman, Iran. Based on the lowest total net present cost (NPC) and excess electricity fractions (fraction of electricity generated in excess of demand and storage capacities that must be dumped), their results showed that PV-battery system was preferred in comparison to wind-battery or PV-wind-battery systems. In a similar study, Asrari *et al.* [39] analyzed the feasibility of hybrid REMG for Binalood, Iran, using HOMER. They evaluated economic aspects of various grid-connected and standalone hybrid REMGs and investigated the feasibility of meeting the reported electricity demand through these

REMGs. As a result, the authors argued that deploying wind-diesel-battery or PV-wind-diesel-battery as standalone hybrid REMGs would be economically and environmentally more feasible than extending the grid lines to the studied location. To study the economic aspects of including storage in a REMG, Al-Badi *et al.* [43] investigated the possibility of using PV with and without batteries for two different villages in Oman to reduce fuel consumption and cost of electricity. The results of this study showed that the combination of PV with existing diesel systems could reduce the cost of electricity from 0.56 to 0.14 USD/kWh. In another study, Ma *et al.* [9] investigated a standalone REMG for a remote island in Hong Kong. The solar insolation and wind data used in this study were the average hourly measured data in 2009, and hourly load profile was synthesized by adding a degree of randomness for different days and months to the base load which was estimated as 250 kWh/day. As a standalone REMG was considered, the electricity generated in excess of the demand and storage capacity was considered to be dumped. The analysis showed that a PV-wind-battery system is optimal and to achieve a 100% RES fraction 48.6% of the total energy produced by the RES would be dumped resulting in a large LCOE of 0.595 USD/kWh, which was three times the current tariff in Hong Kong in 2013. Table 2.1 summarizes the literature reviewed in which HOMER was used.

Table 2.1. Summary of the literature review on RES using HOMER.

Study	Location	Climate	Components	Grid Connected	Measured Data	RES fraction	LCOE USD/kWh
Bekele & Palm, 2010 [41]	Ethiopia Rural area 200 family (1000 inhabitants)	Tropical	PV-Wind-Diesel Generator-Battery	No	Sunshine duration,	51%	0.38
						81%	0.46
Giannoulis & Haralambopoulos, 2011 [11]	Greece Lesvos Island	Mediterranean	Wind-Diesel Generator	No	Wind, Load	--	--
Asrari, Ghasemi, & Javidi, 2012 [39]	Iran Binalood, Sheikh Abolhassan village	Cold semi-arid climate	Wind	Yes	Wind, Solar	31%	0.144
			Wind-Diesel Generator-battery	No	Wind, Solar	31%	0.409
			PV-Wind- Diesel Generator-battery	No	Wind, Solar	45%	0.422
Askari & Ameri, 2012 [40]	Iran Kerman	Arid climate	PV-Battery	No	Wind, Solar, Load	--	--
Bekele & Tadesse, 2012 [42]	Ethiopia Dejen (107710 inhabitants)	Tropical	PV-Wind-Hydro- Diesel Generator-Battery	No	Sunshine duration	72% to 100%	0.10 to 0.16
Al-Badi *et al.*, 2013 [43]	Oman Al Mazyounah	Sub-tropical dry, hot desert [45]	PV-Diesel Generator	No	Wind, Sunshine duration, Load	0.05%	0.128
	Al Mathafa	Sub-tropical dry, hot desert [45]	PV-Diesel Generator-Battery	No	Wind, Sunshine duration, Load	16%	0.144
Ma *et al.*, 2014 [9]	Hong Kong (remote island)	Sub-tropical [46]	PV-Wind-Battery	No	Wind, Solar	100%	0.595

Middle East Technical University Northern Cyprus Campus (METU NCC) is an isolated community located in a rural region on the Mediterranean island of Cyprus. METU NCC has many characteristics that make it a valuable location to develop, test and evaluate REMG technologies, including being an isolated and relatively self-contained community focused on research and education with large solar resources. The present research is part of a larger body of research to develop and deploy REMG technologies at METU NCC. Previously four studies were performed on the feasibility of installing a PV system at METU NCC, and one of these studies included assessing the wind resources as well. Pathirana and Muhtaroglu [47] studied the feasibility of installing a PV power plant at METU NCC based on the monthly averages of the measured Global Horizontal Insolation (GHI) and demand for 2011 considering different PV technologies. They reported that the lowest and highest monthly average demand in 2011 were measured in July and August, respectively. The authors compared the two options of either storing the surplus energy by batteries or selling it back to the grid, and the reported results showed that the PV system size should be about 6 MW to meet the entire demand in August 2011 as the design month. The LCOE for the designed system with and without storage were 0.24 and 0.14 USD/kWh, respectively. In addition, Tariq [48] developed a methodology for sizing grid-connected REMGs with unidirectional metering and applied the method to METU NCC as a case study. The data used in Tariq's study are the measured solar and demand data for METU NCC from June 2013 to May 2014, and Typical Meteorological Year 2 (TMY2) formatted data for METU NCC generated by Meteonorm V6.1 [49]. The results of the study showed that if the objective was to make the system as large as possible under the constraint of minimizing the excess electricity, the recommended PV size is 600 kW; however, if the objective was to maximize the financial benefits, the recommended PV size increased to 1.8 MW. The reported LCOE in Tariq's study was about 0.13 USD/kWh. As the third study on renewable energy resources at METU NCC, Yenen [50] investigated the solar and wind resources at METU NCC based on the measured data for 12 months from June 2013 to May 2014. Yenen compared the results of his PV model with the energy production from an existing 1.3 MW PV power plant about 10 km away from METU NCC, and the difference in annual electricity production was about 4%. In addition, Yenen studied the available wind resources for the same period of time considering a Weibull distribution. In order to estimate the electricity generation from wind energy, Yenen considered three hub heights of 27, 47 and 67 m for the wind turbines, and the resulting capacity factors were 8.98%, 11.44% and 11.12%, respectively. According to Yenen [50], wind energy systems with less than 2 MW capacities were not feasible for METU NCC. As a reference point, the total installed capacity of wind turbines in the Southern part of the island was 144.3 MW and the capacity factor for an existing wind farm in Larnaca, Southern Cyprus, was 13.17% [50], with Larnaca being a coastal city, about 50 km away from METU NCC. In another study, Sadati *et al.* [51], investigated the feasibility of having a PV power plant for METU NCC with two options of batteries and pumped hydro as the storage systems. It is mentioned that given the currently available technologies, it is not economically feasible to create a standalone PV system with energy storage which would make a 100% RES fraction REMG for METU NCC. Moreover, the results of the study showed that it is possible to meet 30% of the demand by PV and battery, and 85% by PV and pumped hydro systems with LCOEs less than the current electricity tariff. Although pumped hydro system resulted in a higher RES fraction, supplying the required amount of water for a campus located on an island was reported to be challenging.

In summary, the feasibility of REMG has been investigated for locations throughout the world including for METU NCC which has many unique characteristics that make it a valuable location for research into REMGs. While these studies investigated the sensitivity of the system's energetic and economic performance as the type and size of key technologies included in the REMG were varied (e.g., PV, wind, diesel and batteries), a REMG design methodology and performance assessment considering the variations in the availability of the renewable energy resources have not been thoroughly investigated. In addition, while a few studies have been performed to specifically investigate the feasibility of REMG for isolated Mediterranean communities including METU NCC [25], [48], [50], [52], none of these studies simultaneously considered the possible inclusion and sizing of PV, wind and energy storage systems.

CHAPTER 3 – METHODOLOGY

The methodology is based on the integration of energetic and economic models that estimate the energetic performance of a PV system, wind turbine, battery bank and PHS along with the NPC and LCOE for the REMG. The energetic model consists of sub-models for the PV and wind systems, battery bank and PHS. Details for each of these models are given in the following subsections.

3.1 PV System Model

The hourly energy output by the PV system is given in Eq. (3.1).

$$E = \eta_{PV} A I_{PV} P_f \tag{3.1}$$

where E is the electrical energy produced, η_{PV} is the PV module efficiency, A is the PV panel area, I_{PV} is the total hourly insolation on the PV panel, and P_f accounts for losses in the system associated with the inverter, wiring, dust and shading on the panel. The PV model is based on the characteristics of the PV panel given by the manufacturer such as the nominal efficiency (η_{ref}), the nominal operating cell temperature ($NOCT$), the panel reference temperature (T_{ref}), the reference hourly insolation for $NOCT$ (I_{NOCT}) and the temperature coefficient of the panel (β_{ref}). The PV module efficiency, η_{PV}, is considered to be variable due to the effect of changes in panel temperature and insolation using Eq. (3.2), which is suggested by Ali *et al.* [37].

$$\eta_{PV} = \eta_{ref} \left\{ 1 - \beta_{ref} \left[T_a - T_{ref} + (NOCT - T_a) \frac{I_{PV}}{I_{NOCT}} \right] \right\} \tag{3.2}$$

where T_a is the ambient temperature. The hourly temperature data for METU NCC are taken from the TMY2 data set described in detail in Section 4.2. In this study for

METU NCC, the specifications for the CS6X-P PV module produced by CanadianSolar Co. are considered [53]. The values of the parameters used in this case study are given in Table 3.1.

Table 3.1. The parameters used in PV model.

Parameter	Value	Reference
η_{ref}	15.88%	[53]
T_{ref}	25°C	[53]
$NOCT$	45±2°C	[53]
I_{NOCT}	800 Wh/m^2	[53]
β_{ref}	0.43%	[53]
P_f	85%	[54], [55]

3.2 Wind System Model

The characteristics of a wind turbine are given by the manufacturer based on experimental measurements and tests. One of the main characteristics is the power output of the turbine versus the wind speed, which includes all the losses associated within the wind turbine. Therefore, it can be considered as a model to estimate the power production from a single wind turbine. The wind turbine selected for this study is the S48 manufactured by GoldWind Co. with 750 kW rated power, since its data including cost are available and the capacity is appropriate for this study. The power curve versus wind speed for the selected wind turbine model is given in Figure 3.1. Additionally, technical specifications of the selected wind turbine are given in Table 3.2 [43].

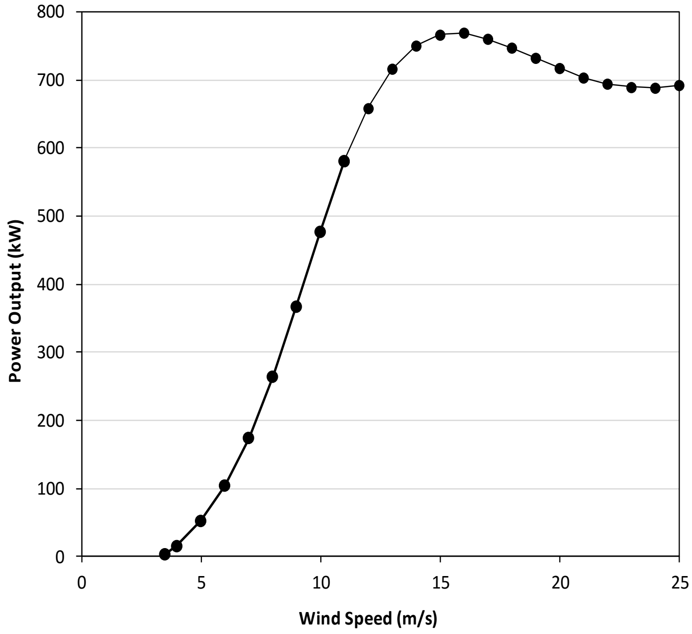

Figure 3.1. Power versus wind speed curve for S48-750 kW wind turbine (adapted from [43]).

Table 3.2. Technical specifications of the selected wind turbine [43].

Parameter	**Value**
Rated Power	750 kW
Hub Height	50 m
Cut-in Wind Speed	3.5 m/s
Rated Wind Speed	14 -15 m/s
Cut-out Wind Speed	25 m/s
Survival Wind Speed	70 m/s

3.3 Energy Storage System Model

In order to estimate the stored energy and required storage size, a model is developed based on the flowchart shown in Figure 3.2. As shown in the flowchart, the excess energy produced by PV system is distributed among short and long-term ESS types.

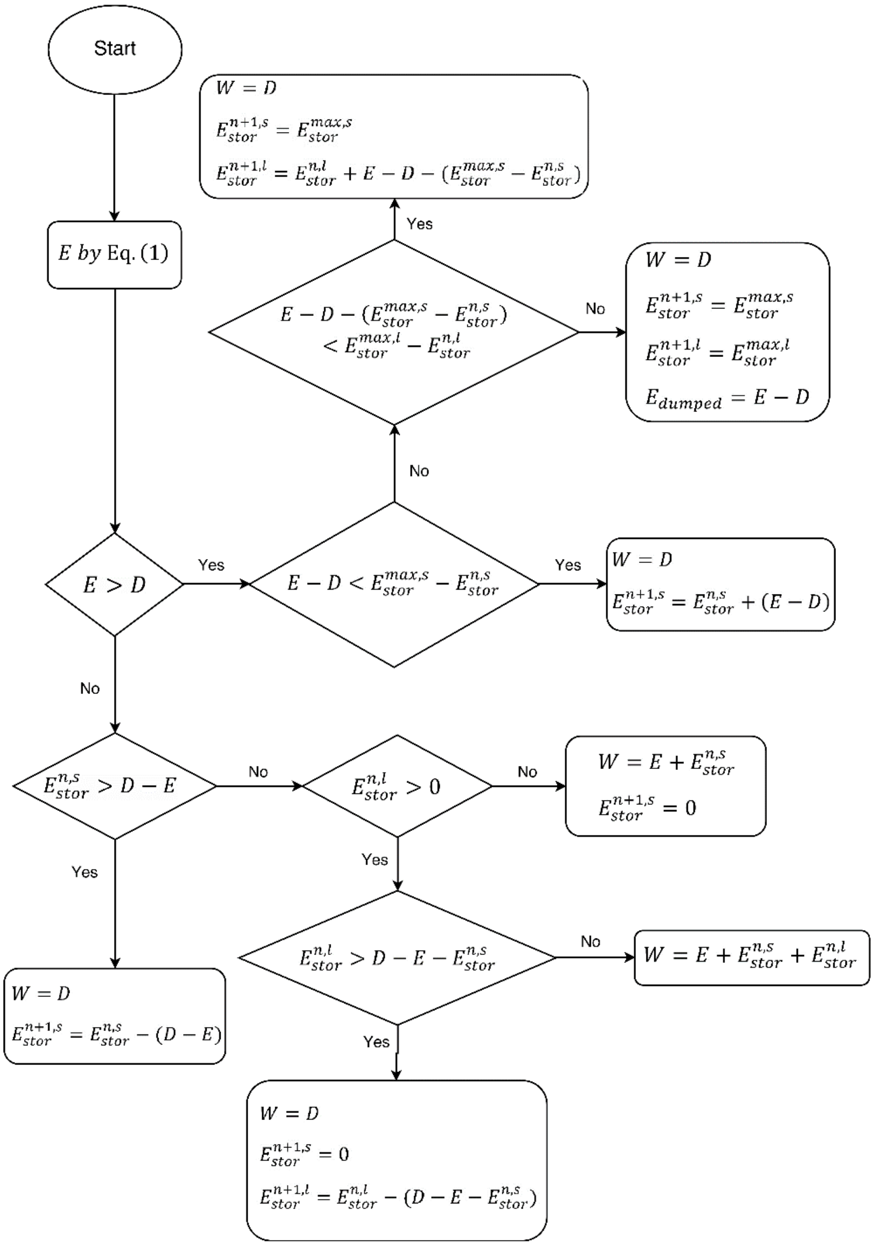

Figure 3.2. Flowchart to determine the output of a REMG consisting PV, short- and long-term ESS.

Among the given parameters in Figure 3.2, the ones with superscript *s* (e.g., $E_{stor}^{n,s}$) refer to short-term and the ones with superscript *l* (e.g., $E_{stor}^{n,l}$) refer to long-term ESS. Moreover, *D* is the demand at time *n*, E_{stor}^{n} is the stored energy at time *n* that is available to be utilized based on the DoD, $E_{stor}^{\max}$ is the maximum capacity of the ESS to store energy, and *W* is the electrical energy output of the REMG. Except for $E_{stor}^{\max}$, all the parameters in Figure 3.2 are time dependent, and they need to be recalculated for each time step.

In order to apply the effect of the round trip efficiency (η_{ESS}), the charge and discharge efficiency of ESS is assumed to be equal to $\sqrt{\eta_{ESS}}$ [22], [35]. Moreover, the batteries are modelled in this study using *kinetic battery model* which is thoroughly described by Jos [22]. This model determines the charging and discharging power limits of the battery at each time step using the state of charge (SoC), rated voltage, and maximum charge and discharge currents. PHS model is adapted from [36] and [35], and its charge and discharge power values are constant for each PHS capacity and independent of SoC unlike battery model. In this study, the minimum size of ZBB is found for this 4-minute delay (1/15 of an hour) by dividing the maximum hourly demand in a year by 15. In case of grid-connected REMGs, this delay can also be covered by the grid; however, for the current study for increasing the possibility of islanding from the grid a minimum size of short-term ESS is considered as stated.

The main characteristics of the ESS which are considered in the current study are depth of discharge (DoD), charge and discharge rates, and round trip efficiency (η_{ESS}). DoD determines the maximum allowed discharge of the ESS. The DoD is about 95% for PHS and varies from 60% to 80% for different types of batteries [15]. In case of batteries, the lifetime of the system depends on the number of cycles that the battery gets fully charged and discharged; therefore, the battery lifetime increases by decreasing the DoD. It is possible to determine the optimum DoD for batteries by minimizing its cost and maximizing the energy output for a given configuration of RES with batteries [31]. Table 3.3 contains η_{ESS} and DoD values for PHS and ZBB used in this study.

Table 3.3. The characteristics of the ESS systems considered in the current study.

Parameter	**ZBB**	**PHS**
Round Trip Efficiency (η_{ESS})	72%	81%
DoD	80%	100%

More details on energy storage system types are given in Appendix A.

3.3.1 Battery Bank Model

The battery bank is a collection of batteries. The battery bank is modeled using kinetic battery model [33] as a device which is capable of storing a certain amount of DC electrical energy with constant round-trip energy efficiency, and limited by a maximum charge and discharge current and a maximum Depth of Discharge (DoD) [63]. The DoD determines the minimum allowed State of Charge (SoC) for the battery in order to maximize its life time. In the current study, an energy balance is applied to the battery in order to determine the available energy in the battery for each hour in the year. The electricity generated in excess of the instantaneous demand will be stored if the battery capacity is not full. Battery lifetime is usually dependent on the DoD and number of charge and discharge cycles. The methods for counting the number of cycles are the same as the methods for counting the load cycles in structural fatigue analyses [44], [64]. In this study the lifetime of the battery is considered constant and independent of the DoD based on the given specifications by the manufacturer [20]. The specifications for the batteries used for this study are given in Table 3.4.

Table 3.4. ZBB specifications used in the model.

Parameter	Value	Reference
Capacity	100 or 1000 kWh	[20]
Round Trip Efficiency	70%	[20]
Max. Charge Current	250 A	[44]
Max. Discharge Current	500 A	[44]
Nominal Voltage	840 V	[44]
Depth of Discharge	20%	[44]
Lifetime	20 years	[20]

3.3.2 Pumped Hydro System Model

Two parameters are assumed for the PHS system and the rest of the system parameters are calculated based on: (i) the maximum energy content of PHS ($E_{stor}^{\max}$) in kWh, and (ii) the time that it takes to fully discharge PHS (t_{out}) in hours. Accordingly, the discharge power for the system (P_{out}) can be calculated by,

$$P_{out} = \frac{E_{stor}^{\max}}{t_{out}} \tag{3.3}$$

where P_{out} is the power that can be produced by the generator. The water volume required for having a storage capacity equal to $E_{stor}^{\max}$ would be found by,

$$P_{out} = \rho g h \eta_{out} \frac{V}{3600 t_{out}} \tag{3.4}$$

where ρ is the density of water, g is the gravitational acceleration, h is the water head, i.e., the distance between upper and lower reservoirs, η_{out} is the efficiency of the turbine generator, and V is the volume of the water required to generate P_{out}. Assuming that the charging pump has a known power (P_{in}) and efficiency (η_{in}), the flow rate of the water for charging PHS (Q_{in}) can be calculated by,

$$Q_{in} = \frac{P_{in}}{\rho g h \eta_{in}} \tag{3.5}$$

and the required time (t_{in}) and total energy (E_{in}) to fully charge PHS can be found by,

$$\begin{aligned} t_{in} &= \frac{V}{Q_{in}} \\ E_{in} &= P_{in} t_{in} \end{aligned} \tag{3.6}$$

In the current study, it is assumed that P_{in} = P_{out} and η_{in} = η_{out} [35]. Finally, the roundtrip efficiency of PHS (η_{PHS}) would be calculated by Eq. (3.7).

$$\eta_{PHS} = \frac{E_{stor}^{\max}}{E_{in}} \tag{3.7}$$

3.4 Energetic Performance System Model

As the preliminary sizing step for REMG, the technical performance of different PV system and ESS capacities for REMG is evaluated based on RES fraction and Capacity Factor (CF) which are calculated by Eq. (3.8), (3.9).

$$RES \quad Fraction = \frac{Annual \quad Energy \quad Met \quad by \quad RES}{Annual \quad Demand} \tag{3.8}$$

$$CF = \frac{Annual \quad Energy \quad Generated \quad by \, RES}{Installed \quad Capacity \quad of \quad RES \times Time} \tag{3.9}$$

These parameters calculated for the different sizes of the REMG components and the results are given in the following section.

3.5 Economic Model

The economic performance of the system is assessed using LCOE and NPC. LCOE is calculated as in Eq. (3.10) [56] as,

$$LCOE = \frac{I + \sum_{t=1}^{n} (M_t + F_t) / (1+r)^t}{\sum_{t=1}^{n} E_t / (1+r)^t} \tag{3.10}$$

where I is the initial investment, M_t is the annual maintenance cost, F_t is the annual fuel cost, E_t is the annual energy produced, r is the annual discount rate, and n is the lifetime of the system in years. The annual maintenance cost is assumed to be 1.5% of the initial cost of each component [56]. There is no annual fuel cost for the components included in the designed REMG; however, the annual cost of electricity purchased from the grid is included in the total cost for meeting the entire demand. Additionally, the NPC is calculated using Eq. (3.11), which accounts for costs of initial capital, replacement, operation and maintenance using the discount factor for the cash flow (C_t) over the lifetime of the system. NPC does not directly depend on the energy generated by the REMG, unlike LCOE; therefore, NPC makes a better representative to compare the economic feasibility of different configurations for the REMG. LCOE directly depends on the generated energy and whether one considers or ignores the excess electricity in the calculation of LCOE might lead to significant differences in its resulting value.

$$NPC = \sum_{t=1}^{n} \frac{C_t}{(1+r)^t} \tag{3.11}$$

The values for n and r are considered to be 25 years and 9%, respectively, as suggested by [17], [56]. Considering a 6% inflation rate on average [57] would make the real discount rate 2.83%. The installation costs and lifetimes of the components used in the design of the system are given in Table 3.5. The salvage value that represents the price of the components which would be available for sale or could be utilized further at the end of the RES lifetime is also considered in the NPC for the current study. The corresponding salvage values are calculated based on a linear relation between the remaining lifetime of the component and its depreciation.

Table 3.5. Installation cost and lifetime of the components.

Component	**Cost**		**Lifetime (years)**	**Reference**
PV System	3000	USD/kW	25	[58], [56]
Inverter	700	USD/kW	15	[59], [60]
Wind Turbine	721.6	USD/kW	25	[43]
Battery	300	USD/kWh	20	[20], [25]
Grid Electricity Tariff	0.175	USD/kWh	25	[61]

3.6 Hybrid PV-Battery-PHS Model for REMG

The introduced model for PV is integrated to battery and PHS models as the short- and long-term ESS to form a REMG. The energy generated by PV is used to meet the demand and if in any time step excess electricity is available the battery and then the PHS are charged. In case the electricity generated by PV is not enough to meet the demand, the availability of energy in both ESS is controlled and electricity is provided to cover the demand. The analyses are performed for a range of PV, battery and PHS capacities and the resulting NPC, LCOE and RES fractions are calculated for each case. Amongst the different REMG configurations, the ones with the lowest NPC are selected for further investigation in order to suggest the preferred configuration. For instance, it is recommended that there should be a battery unit in the design for handling urgent needs for the power since there is approximately 4-minute delay in utilizing the power generated by PHS [22].

3.7 Hybrid PV-Wind-Battery Model for REMG

The components of the system which are considered for the current study are illustrated in Figure 3.3. As a case study, the hourly demand for METU NCC is given as the load, and the components for this system are PV panels, wind turbines, inverters and batteries. The system is connected to the grid to supply the fraction of the demand which is not supplied by the RES.

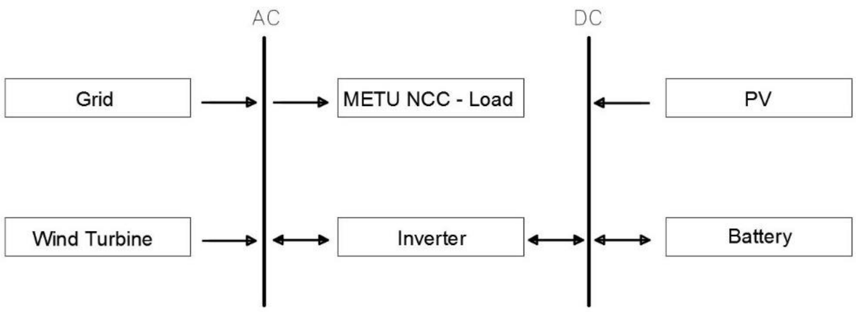

Figure 3.3. Possible system components of a grid-connected hybrid PV-Wind-Battery REMG considered in this study.

This hybrid REMG is modeled in HOMER which uses the energetic and economic models given in the previous sections. HOMER simulates the considered energy system in the given time step by making an energy balance in which the energy demand and available energy production are compared. For the current study, these calculations are done for any system configuration using the possible components given in Figure 3.3, and the economic feasibility of the system is checked to see whether any configuration including RES can meet the demand with a lower NPC than meeting the entire demand only with the grid. HOMER considers initial capital costs of each component and calculates NPC and LCOE for each possible configuration. The configurations can be sorted based on resulting NPC, LCOE or initial capital cost for the given capacity ranges of each component. In this study, all the systems are ranked based on NPC which reflects the total present cost of the system over its lifetime. In the current study, a grid-connected REMG including one or more of PV system, wind turbines and batteries is evaluated to find the lowest NPC.

CHAPTER 4 – CASE STUDY: METU NCC

In this chapter, an overview of METU NCC is presented followed by the data sets for the solar and wind resources and electricity demand of the campus used in this study. The potential for having PHS is also discussed here.

METU NCC is located in the northern part of the island of Cyprus and has a typical Mediterranean climate with hot sunny summers. The average daily global horizontal insolation (GHI) in a year at northwest Cyprus, where METU NCC is located, is 5.48 kWh/m^2 [65] which is comparable with the maximum average daily GHI in a year at Spain (5.35 kWh/m^2), USA (6.03 kWh/m^2) and South Africa (6.43 kWh/m^2) [65]. In Figure 4.1 the availability of GHI for different regions of Cyprus is shown. This shows the high potential for installing solar energy systems at northwest Cyprus. However, the main sources of supplying the demand in the island including the demand for METU NCC are the oil based generators which are polluting the environment and depend on the imported oil.

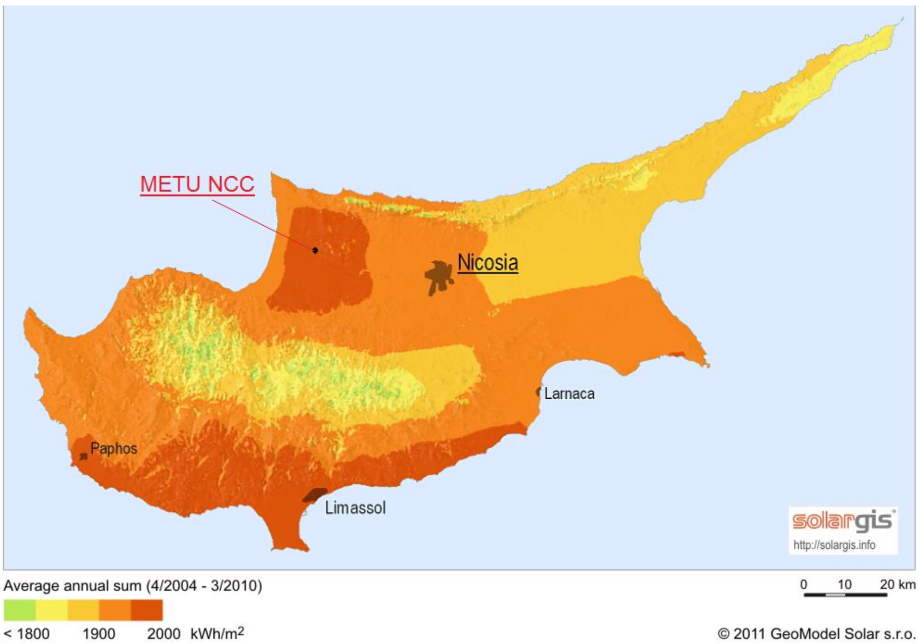

Figure 4.1. Average annual GHI in Cyprus from 2004 to 2010; adapted from [65].

METU NCC is a good example of an isolated community with significant electricity demand and renewable energy resources. Currently, this campus has approximately 2650 students and 270 faculty members and staff, with approximately 70% of these living on campus. Therefore, METU NCC is a fairly self-contained university community with electricity demand for 24 hours per day, 7 days per week. The electricity demand of the campus is mainly supplied by the grid which is almost exclusively generated using imported fuel oil based steam and diesel generators installed on the island, which decreases energy security and results in relatively high electricity costs and significant greenhouse gas emissions and pollution. The northern part of the island has an unstable small grid and during the frequent blackouts, the campus uses diesel generators as a back-up electricity supply, which is also expensive and results in significant local environmental and noise pollution.

METU NCC is currently establishing a REMG for many reasons including economic and environmental, and to support educational activities and research programs. The long term goal for this initiative is to establish a smart grid at METU NCC as a test case for community-level smart grid technologies. The development of this REMG is also part of a larger initiative to strengthen METU NCC's role as a model "green campus". Currently the utilization of micro-grids on the island is limited by uni-directional metering, available land, and a relatively weak grid. Uni-directional metering means that any electricity produced by the REMG in excess of the demand and storage capacities would be fed to the grid for free, and therefore, producing excess energy would not be economically beneficial for the campus. Uni-directional metering can be contrasted with net-metering, feed-in-tariffs, and similar schemes where the institution can benefit economically by supplying excess electricity to the grid. The development of a REMG at METU NCC has been occurring systematically for several years. Solar resources at METU NCC have been monitored with a pyranometer for measuring the global horizontal insolation (GHI) since January 2010 and a pyrheliometer for measuring the direct normal insolation (DNI) since June 2013. In addition, wind resources have been measured at heights of 2, 30, 40, 50 and 60 m since March 2013. In February 2016, a 1 MW PV power plant was commissioned on the campus, with 1 MW being approximately equal to the campus's average electrical power demand.

4.1 Potential for PHS at METU NCC

Although there are no rivers in northern part of Cyprus, there are two manmade reservoirs close to METU NCC which enables the possibilities for PHS. First possibility is to utilize a reservoir almost 2 km away from the campus as the lower reservoir and building an upper reservoir in the campus as shown in Figure 4.2. However, its available water may not be enough for this purposes for all the seasons.

Figure 4.2. Akdeniz reservoir almost 2 km away from METU NCC.

Second possibility is using sea water for PHS and building an upper reservoir at METU NCC as shown in Figure 4.3. However, the distance from the sea would be a problem as the height difference between the sea and the highest location in campus is about 100 m, and it might not be possible to utilize the stored energy in the pumped water for reproducing electricity.

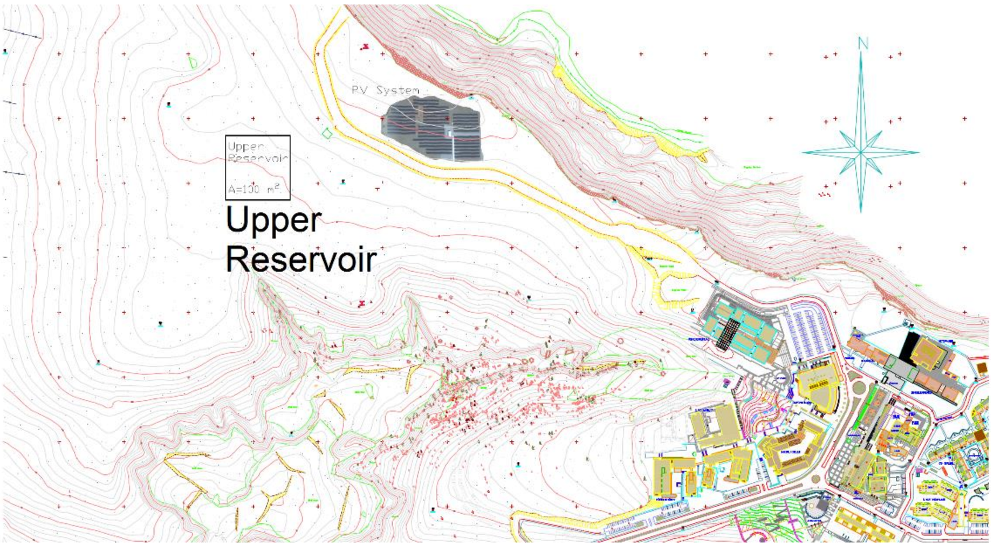

Figure 4.3. It is possible to build an upper reservoir in METU NCC at the location shown by the square.

As the third possibility, using Gecitkoy reservoir as the lower one and building an upper reservoir at the construction site of the dam, at the west side, would be possible as shown in Figure 4.4 and Figure 4.5; however, detailed study should be performed on this construction. The third possibility seems the most feasible one since the water head is about 150 m, and the lower and upper reservoirs are only 2 km away from each other. This possibility requires arrangements with the local island grid authorities since the PHS would be away from the campus and if excess electricity from a REMG at METU NCC is used for charging the PHS at the site the island grid should also be involved.

Figure 4.4. Gecitkoy reservoir, almost 10 km away at the north side of METU NCC.

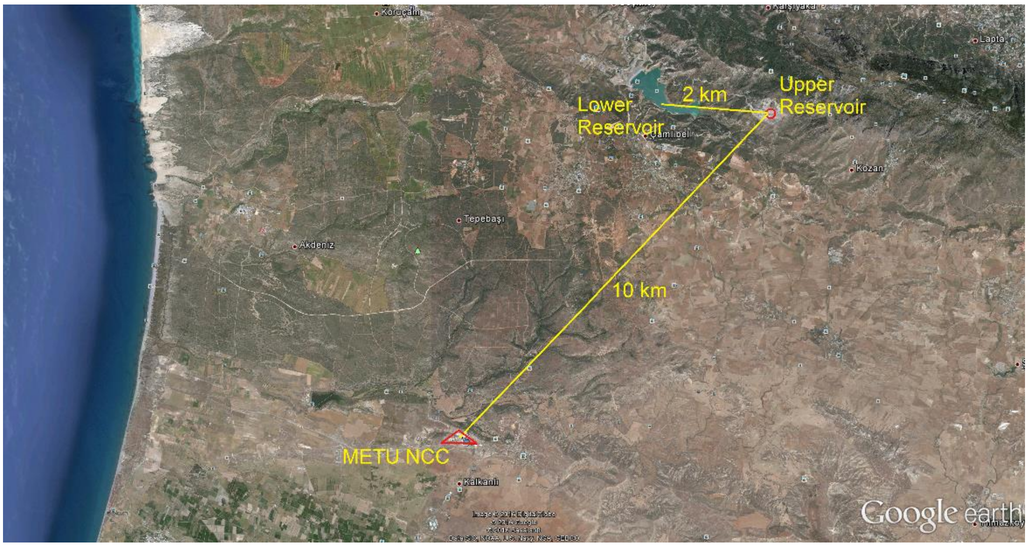

Figure 4.5. Gecitkoy reservoir and possibility of having lower and upper reservoirs

4.2 Resource Data Sets for METU NCC

The performances of PV and wind systems directly depend on the solar and wind resources at the site of the installations. Therefore, when these resources as actual or observed data sets differ from the TMY data set, actual performances deviate from the predicted ones. In this work, four solar resource and two wind resource models are considered as follows.

4.2.1 Solar Resource Data Sets

Two data sets are used as the available solar resources. One set is hourly data created by Meteonorm [49]. The other set is GHI data measured at METU NCC for 2010-2014. These data sets are used to construct four solar resource data sets named and defined as follows:

1. *TMY GHI*: TMY stands for Typical Meteorological Year, and is a model for the meteorological conditions of a "typical" year based on long term measured data. While measured TMY data are not available for METU NCC, a synthetic TMY data set for every hour in a year was generated using Meteonorm (MN) V7.1 software published in 2015 [49]. Note that there are reports of differences between GHI data sets for the same locations generated by different versions of MN [66], [67]. MN V7.1 is marketed as being the most reliable on the date of this study is conducted as the models and data collections have been improved and updated relative to the older versions [66].
2. *Average Measured GHI*: GHI has been measured at METU NCC since January 2010 using a Kipp&Zonen (CMP22) pyranometer. These data were averaged over five years to yield the *Average Measured GHI* data set.
3. *Large Measured GHI*: Among the five years of measured GHI, the year 2013 had the largest annual average daily value. Thus, this data set is used as an estimated upper bound for predictions compared to other available data sets, although it may not reflect the maximum possible insolation for METU NCC at all hours. The annual average daily GHI measured in 2013 is 7% higher than the annual average daily value for GHI given in the TMY data.
4. *Small Measured GHI*: Among the five years of measured GHI, the year 2014 had the lowest annual average daily value. This data set is used as an estimated

lower bound for predictions compared to other available data sets, although it may not reflect the minimum possible insolation for METU NCC at all hours. The annual average daily GHI measured in 2014 is 19% less than the annual average daily value for GHI given in TMY data.

TMY data sets have been shown to be the most reliable solar resource data sets for designing solar energy conversion systems [68]. Herein the *TMY GHI* is used to design the system and characterize a nominal system performance, which will deviate from the actual system performance due in part to differences between the *TMY GHI* and actual solar resources. The measured data sets provide the opportunity to compare predicted performance between TMY and measured data sets. To qualitatively assess the consistency of these data sets, the average daily resources for each month for all 4 data sets are plotted in Figure 4.6. As shown in Figure 4.6, overall the *TMY GHI*, *Average Measured GHI*, and *Large Measured GHI* data sets show good consistency. The *Small Measured GHI* data set predicts about 19% and 25% lower solar resources on annual average than the *TMY GHI* and *Large Measured GHI*, respectively. The *Small Measured GHI* and *Large Measured GHI* data sets are only used to examine the performance of the designed REMG for METU NCC as the solar resource data sets are varied. Therefore, the comparison of the system performance under design and off-design conditions will give some indication of the robustness of the suggested design given the possibility of variabilities in the solar resources.

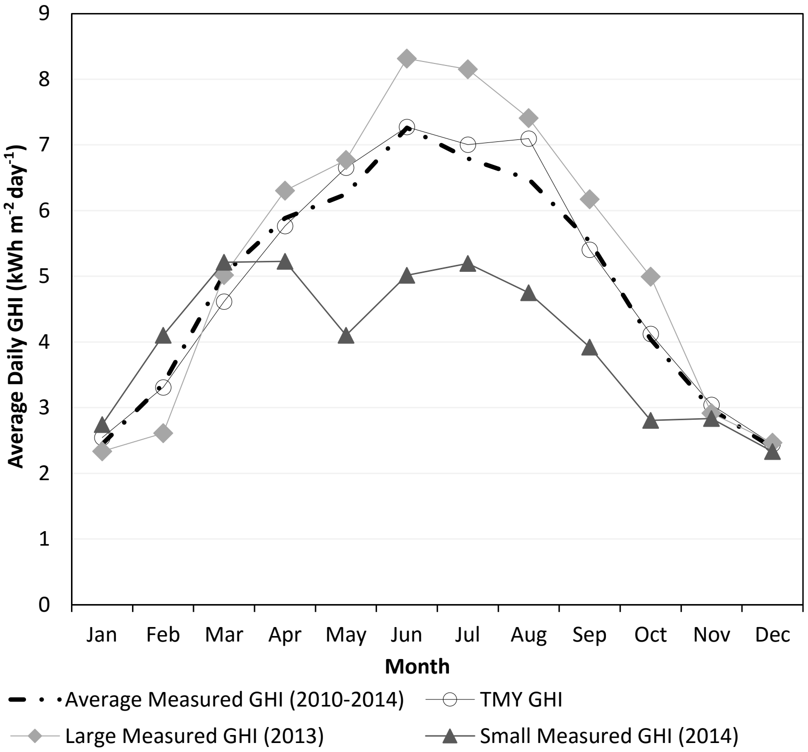

Figure 4.6. Average daily values for each month for *Average Measured GHI* (2010-2014), *TMY GHI*, *Large Measured GHI* (2013) and *Small Measured GHI* (2014).

There are different methods for estimating the global insolation on any given surface with desired orientation [69]. Herein the diffuse insolation is calculated from GHI using the sky clearness method in order to find the global insolation on any given tilted surface. This method is presented by Duffie and Beckman [69] and is based on the hourly clearness index (k_T) calculated as the ratio of GHI (I) and the extraterrestrial horizontal insolation (I_o).

$$k_T = \frac{I}{I_o} \tag{4.1}$$

The clearness index is a dimensionless number between 0 and 1 indicating the fraction of the extraterrestrial insolation which succeeds to strike the surface of the earth. The clearness index is used for calculating the diffuse horizontal insolation (DHI) based on empirical relations [70], and GHI and DHI are used to calculate DNI by the formulation given in [69]. DHI, DNI, the orientation of the PV module defined by its tilt and azimuth angles and the position of the sun in the sky defined by its zenith and solar azimuth angles are used to find solar insolation on the PV module (I_{PV}) [69].

For the case study for METU NCC, I_{PV} is modeled for four characteristic surfaces of fixed-tilted (FT), East-West (EW) tracking, North-South (NS) tracking, and two-axis (2A) tracking defined as follows. A FT surface faces due south and is fixed at a 25-degree tilt angle which maximizes the total annual solar insolation on the surface for METU NCC based on the analyses for this study. EW tracking tracks the sun from East to West about a horizontal North-South axis, whereas NS tracking tracks the sun from North to South about a horizontal East-West axis. 2A tracking tracks the sun about 2-axes, and the surface is always normal to the sun-earth line. In Figure 4.7 the predicted global insolation on these surfaces using the TMY data set for METU NCC are presented. As shown in the figure, 2A tracking system has the highest average daily total insolation for all the months among the four surface considered. Moreover, EW receives higher insolation than NS and FT surfaces from March to October which results in greater annual average insolation for EW compared to NS and FT. Considering the higher complexity and higher cost of the 2A tracking system relative to EW tracking with only a 9% increase in annual energy output, the EW tracking system is preferred in this study along with the FT surfaces.

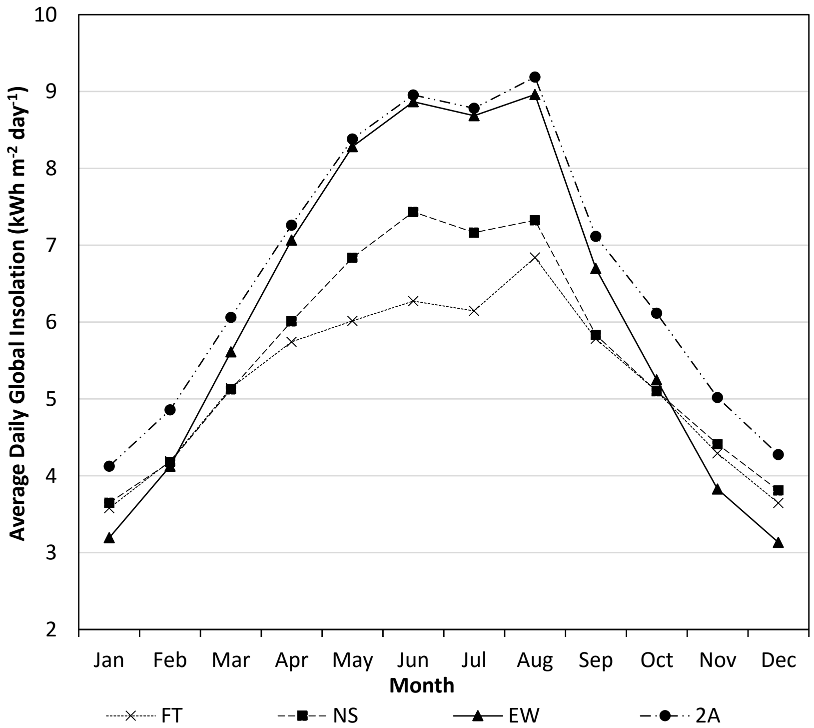

Figure 4.7. Available average daily global insolation for each month at FT, EW, NS and 2A tracking surfaces.

4.2.2 Wind Resource Data Sets

Four wind resource data sets are available for METU NCC named and defined as follows:

1. *TMY Wind*: Hourly wind speed data given in the synthetic TMY data generated by MN V7.1 for METU NCC and corrected for 50 m above ground level as described below.
2. *2014 Measured Wind*: The hourly wind speed data measured at 50 m for METU NCC in 2014.
3. *2015 Measured Wind*: The hourly wind speed data measured at 50 m for METU NCC in 2015.

As for the solar resources, the *TMY Wind* data set is used to design the REMG and predict its nominal performance. To examine the predicted performance of REMG using the measured data for wind, *2014 Measured Wind* and *2015 Measured Wind* data sets are used as only these two complete year data are available

In this study and as often occurs when designing RESs, measured wind data are only available for a short period of time, and the TMY data set is expected to provide a more reliable wind speed data than short term measured data. The wind speed given in the TMY data set are for an elevation of 10 m which is converted to the wind speed at the wind turbine hub height at each time step using Eq. (4.2) [17], [71].

$$\frac{U_{hub}}{U_{anem}} = \left(\frac{Z_{hub}}{Z_{anem}} \right)^{\alpha} \tag{4.2}$$

where U_{hub} is the wind speed at the hub height of the wind turbine, U_{anem} is the wind speed at the anemometer height, Z_{hub} is the hub height of the wind turbine, Z_{anem} is the anemometer height, and α is the power law exponent which is assumed 0.14 for this study [37]. In the present work, the hourly wind speed at the height of 10 m in the TMY data set is converted to the wind speed at the wind turbine hub height of 50 m and is input to HOMER as the wind resources.

Figure 4.8 illustrates the average daily wind speed for each month for the *TMY Wind* data at 50 m, and the measured data at 50 m in 2014 and 2015. The average wind speed is increased by about 25%, when the wind speed in the *TMY Wind* data set is converted to the height of 50 m using Eq. (4.2). As shown in Figure 4.8, the average wind speed given by *TMY Wind* data set is lower than the measured wind speed for both 2014 and 2015. Therefore, using *TMY Wind* data set would be more conservative in terms of predicting the energy production from a wind turbine.

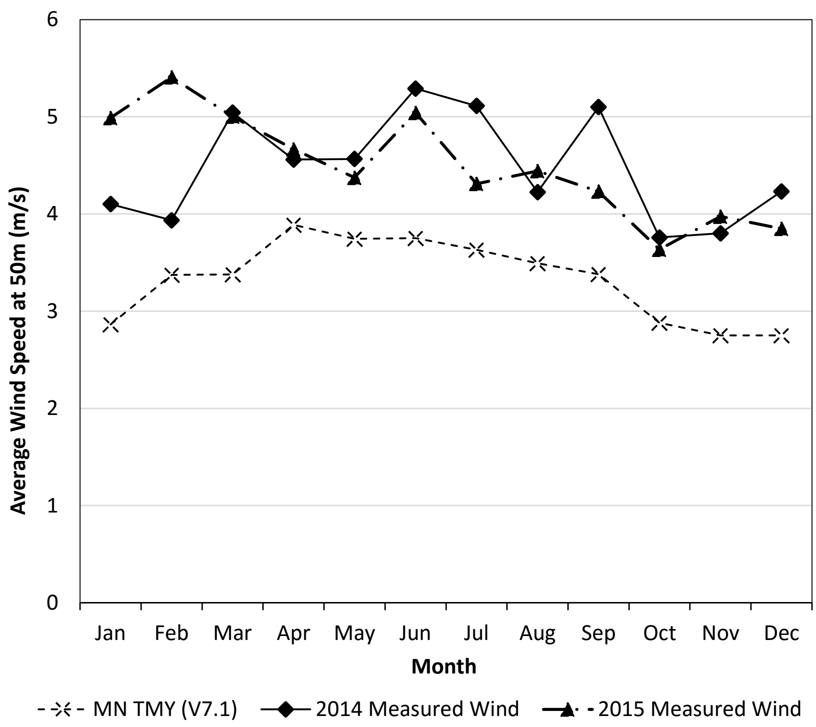

Figure 4.8. Average wind speed at 50 m from *TMY Wind*, *2014 Measured Wind* and *2015 Measured Wind* at METU NCC.

4.2.3 Demand Data Sets

One of the main inputs to the given model is the demand data. As a first approximation, any relation between the solar and wind resources and electricity demand is neglected; therefore, the solar and wind resource and the demand data sets are not coupled. Approximately 35% to 40% of the electricity consumption of METU NCC is associated with the predominately undergraduate student population, including educational activities, dormitories, etc. [72]. The hourly electricity demand data from June 2013 to May 2015 for the campus were obtained from the local authority of the electricity grid for the northern part of the island (Kib-Tek) and is termed the *Hourly Demand* data set. The monthly demand was obtained from university billing records from 2011 to the present and is termed the *Monthly Demand* data set. The average daily electricity demand for METU NCC was obtained from the

Hourly Demand data set by averaging the demand for each day over two years from June 2013 to May 2015 and is shown in Figure 4.9. The campus population varies significantly throughout the year, and the effect of population on electricity demand is clearly seen in Figure 4.9. The campus population is the highest from September to January (fall semester) and from February to June (spring semester), is slightly lower during summer school in June and July and during the winter break in late January and early February, and decreases significantly between the summer and fall terms from August to mid-September, when there are practically no students on campus and much of the academic and support staff are on vacation. Additionally, the campus has a large air-conditioning load as seen by the large electricity demand in June and July and the sharp peak in September when students return for the fall semester. In contrast, the main heating system is based on fuel oil and not electricity; therefore, the heating in winter does not affect the electricity demand significantly.

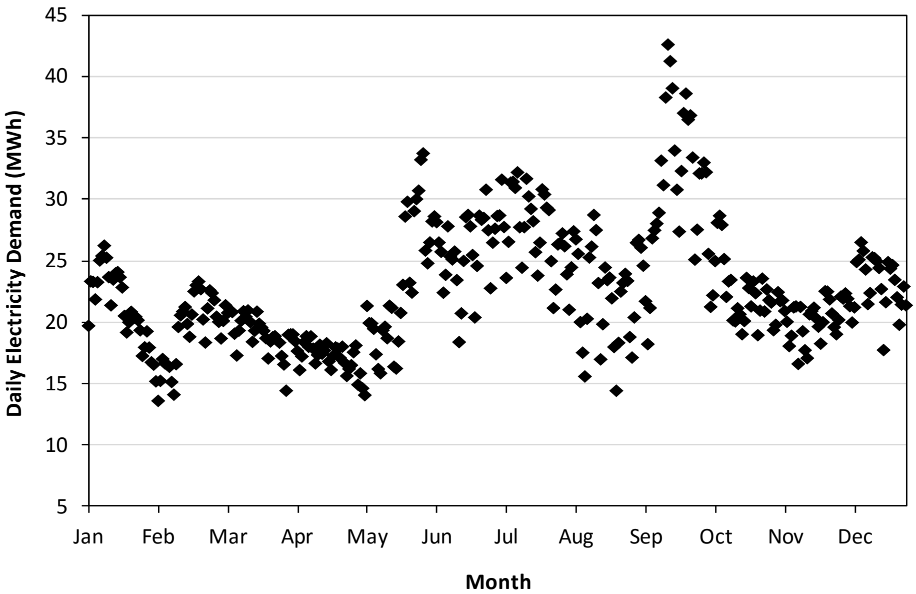

Figure 4.9. Average daily demand for METU NCC calculated by averaging the demand for two years from June 2013 to May 2015.

Because METU NCC is a relatively new and growing campus, its electricity demand is expected to increase significantly over the lifetime of the REMG. Therefore, a model for the demand growth is necessary to properly design the REMG. Using the *Monthly Demand* data set from 2011 to 2014 and the model presented by Ali [72], the demand growth for METU NCC is predicted. Ali [72] used both the linear regression and Holt's methods, and the results for these two methods were consistent. Herein the linear regression method results are used. To easily adapt this demand model to the present work and as a first approximation, the REMG is assumed to be installed in 2014 and have a lifetime of 25 years, and therefore, 2026 is the midpoint in the design lifetime. The demand predicted in 2026 is then used as the input to design the REMG.

To illustrate how the demand is growing with time, Figure 4.10 presents the average daily demand for each month for 2011 based on the *Monthly Demand* data set, and from June 2013 to May 2015 derived from the *Hourly Demand* data set, and the predicted demand for 2026.

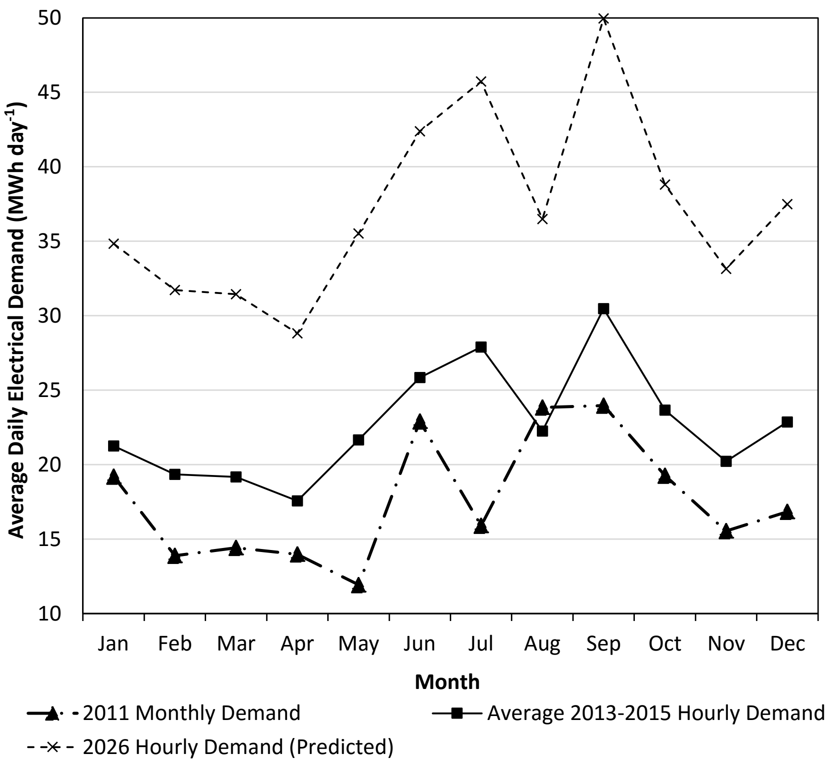

Figure 4.10. Average daily demand for each month for the available data sets: 2011 Monthly Demand provided by METU NCC administration, Average 2013-2015 Hourly Demand provided by Kib-Tek and Hourly 2026 Demand predicted for METU NCC.

CHAPTER 5 – RESULTS AND DISCUSSIONS

The given methodology is applied using the data for METU NCC, and the results are given in the following subsections in terms of the proposed REMG configuration and its economic and technical performance including the LCOE, NPC, RES fraction, excess energy, energy output from each component, estimated reduction in CO_2 emissions and the results for the sensitivity analyses to resource data sets. The excess electricity is classified as being either *donated* or *dumped*. Donated electricity corresponds to electricity flowing to the grid for free due to the uni-directional metering employed at METU NCC. Dumped electricity corresponds to electricity produced by RES that exceeds the inverter capacity and cannot be stored, and therefore is dumped.

5.1 Verification of the Developed Model with HOMER

The PV and ESS model results are verified using the results of the similar configurations modeled in HOMER. Table 5.1 contains the results for four cases of PV and battery sizes with the same inputs. As it can be seen from the table, the RES fractions are identical, and the difference in the NPC values are negligible. The LCOE values are not compared since the method used by HOMER to calculate LCOE is different. HOMER assumes that all the excess electrical energy is utilized by the grid connected to the REMG. Although this energy is donated to the grid for free, it makes the denominator of Eq. (3.10) to be larger and the resulting LCOE to be smaller. Therefore, only RES fractions and NPC values are compared in Table 5.1. It should be noted that the cases shown in Table 5.1 are for PV systems with 0 tilt angles and are modeled only for the comparison of the results of the developed model and

HOMER results. They are not expected to be used as a reference for any other applications.

Table 5.1. NPC and RES fractions resulted from the developed model and models in HOMER for verification of results of the model developed for this study.

PV (MW)	Battery (MWh)	DoD (%)	HOMER-RES fraction (%)	Developed Model-RES Fraction (%)	HOMR-NPC (USD)	Developed Model-NPC (USD)	Difference in NPC (%)
2	0	-	21	21	39.2M	39.4M	0.56
2	1	80	21	21	39.6M	39.7M	0.20
10	0	-	47	47	52.1M	52.7M	1.15
10	10	100	68	68	47.2M	47.1M	-0.25

5.2 Case 1: Hybrid REMG Consisting PV-Battery-PHS

The results for Case 1 are given in two sub-sections. The first section contains the estimated performance of currently installed PV system which does not include any ESS. The second section contains the effects of deploying short- and long-term ESS on establishing a hybrid REMG which technically would be feasible and economically would have the lowest NPC among the studied REMG configurations.

5.2.1 Current PV system at METU NCC

The NPC of meeting the electricity demand for METU NCC for 25 years, termed as NPC_{grid}, is estimated to be 42.2M USD considering the electricity tariff in 2015 which was 0.175 USD/kWh. The results of the current study indicate that the installed PV system at METU NCC which is 1 MW would decrease the NPC to 40.59M USD. Table 5.2 includes the NPC, LCOE, RES fraction and *avoided NPC* considering different PV system sizes. The avoided NPC is the difference between NPC of the given PV system and NPC_{grid}.

Table 5.2. NPC, LCOE, RES fraction and avoided NPC results for different PV system sizes.

PV (MW)	NPC (USD)	LCOE (USD/kWh)	RES fraction (%)	Avoided NPC (USD)	Avoided NPC (%)
1	41.43M	0.172	11.32	0.77M	1.82%
1.5	41.06M	0.169	16.95	1.14M	2.70%
2	40.77M	0.169	22.38	1.43M	3.39%
2.2	40.72M	0.169	24.42	1.48M	3.51%
2.3	40.70M	0.169	25.40	1.50M	3.55%
2.4	40.70M	0.169	26.35	1.50M	3.55%
2.5	40.71M	0.169	27.27	1.49M	3.53%
2.6	40.74M	0.169	28.16	1.46M	3.46%
3	40.96M	0.170	31.44	1.24M	2.94%

For the studied range of PV sizes, which is from 100 kW to 6 MW with 100 kW increments, the NPC of meeting the electricity demand is lower than NPC_{grid}, which shows that deploying a PV system that partially covers the demand is economical for this community. The lowest NPC is estimated for a PV system with a capacity of 2.4 MW; however, a 1 MW system was installed at METU NCC because of the regulations at Northern Cyprus. Currently, the regulations do not allow the two-way tariff in Northern Cyprus.

5.2.2 Hybrid REMG with Energy Storage at METU NCC

The minimum size of short-term ESS (ZBB) for METU NCC with the estimated maximum hourly demand of about 4.1 MWh would almost be 0.27 MWh considering that ZBB is desired to be capable of cover the demand during the 4-minute delay in starting PHS as described in Section 2. For the current study, this minimum size is considered as 0.30 MWh to cover the possible uncertainties in estimating the maximum hourly demand. The study is conducted for a range of 0 to 8 MW with 0.1 MW increments for PV system, 0.3 to 2 MWh with 0.1 MWh increments for ZBB and 0 to 35 MWh with 0.5 MWh increments for PHS. The results of NPC, LCOE, RES fraction and avoided NPC for REMG configurations are sorted in ascending order of NPC. NPC, LCOE, RES fraction and avoided NPC are shown for four different configurations in Table 5.3. Configuration 1 resulted in the lowest NPC among the studied configurations in the search space; however, the required water for PHS in this configuration, which is about 20,000 m^3, seems to be unavailable for METU NCC. Therefore, two other configurations are also presented for which the required amounts of water are estimated to be available in nearby reservoirs of METU NCC. Configurations 2 and 3 require about 10,000 m^3 of water. As shown, all these configurations have NPC lower than NPC_{grid} which means it is more economical to establish a REMG than using the grid for covering the entire demand. Moreover, deploying ZBB increases the NPC therefore in configurations 1 and 2 which have the lowest NPC values the ZBB size is zero. Nevertheless, the suggested size of ZBB for configurations 3 and 4 is the minimum possible size for the short-term ESS in this study which is very small comparing to the size of the long-term ESS (PHS) since the cost per unit energy of ZBB is four times higher than the one for PHS. The required water for configuration 3 is more likely to be available at the campus and a minimum of ZBB is considered in this configuration which increases the possibilities of islanding from the grid; therefore, configuration 3 is considered as the preferred design for the hybrid REMG. By deploying this configuration, it is estimated that the REMG can meet the demand for 8.92% of the hours in a year and 2650 tons of CO_2 emissions would be avoided. Nevertheless, more detailed studies on the land area, installation costs, evaporation rate, etc. should be conducted as the future studies.

Table 5.3. Selected results with minimum NPC at each studied range for PV and ESS capacities.

Configuration No.	Short ESS (ZBB) (MWh)	Long ESS (PHS) (MWh)	PV (MW)	NPC (USD)	LCOE (USD/kWh)	RES fraction (%)	Avoided NPC (USD)	Avoided NPC (%)
1	0	5.5	3.1	40.62M	0.168	34.05	1.58M	3.74
2	0	2.5	2.7	40.65M	0.168	29.72	1.55M	3.67
3	0.3	2.5	2.7	40.65M	0.169	29.78	1.55M	3.67
4	0.3	5.5	3.1	40.77M	0.169	34.07	1.43M	3.39

The annual predicted demand for METU NCC and energy generated by the REMG with 0.3 MWh ZBB and 2.5 MWh PHS are shown in Figure 5.1. As it is shown, for the system of configuration 3, the dumped energy is negligible and the annual energy used from both ESS, which is the difference between “Energy by PV” and “Energy by PV+ESS” is approximately 230 MWh which is about 1.7% of the demand. The utilized energy from ESS increases for PV capacities higher than the one in configuration 3 (2.7 MW); however, the marginal cost of electricity generation by PV+ESS and consequently the NPC for hybrid REMG also increases. This can be explained better by Figure 5.2 in which the CFs for the cases of *produced* and *utilized* energy are shown. *Produced* energy is the total energy that is generated by PV system and *utilized* energy is the fraction of the produced energy which is used to meet the demand and the dumped energy is subtracted from it. CF of a PV system without considering any ESS and any dumped energy would be about 20.7%. Deploying ESS increases CF; however, if the dumped energy is also considered in the calculation of CF, the resulting CF would decrease dramatically. This shows that the investment for higher PV capacity does not pay off in monetary terms which is the reason for higher marginal cost of electricity for a REMG with configuration 3.

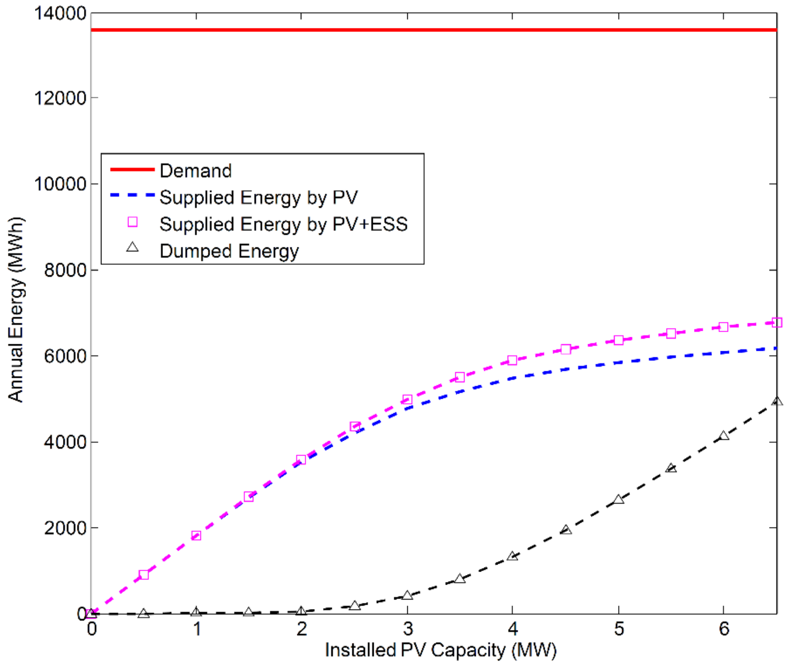

Figure 5.1. Annual demand for METU NCC and annual energy generated by REMG with 0.3 MWh ZBB and 2.5 MWh PHS for different PV capacities.

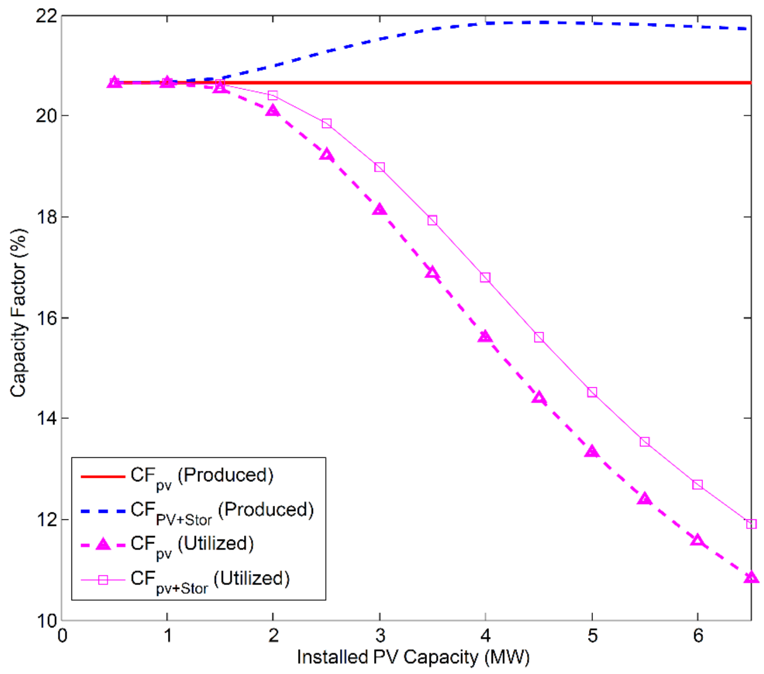

Figure 5.2. Capacity factor for the REMG with 0.3 MWh ZBB and 2.5 MWh PHS for different PV capacities.

The LCOE of the generated electricity by a REMG with 0.3 MWh ZBB and 2.5 MWh PHS for different PV system capacities is shown in Figure 5.3. LCOE also increases dramatically when the PV capacity increases after the capacity of 2.7 MW.

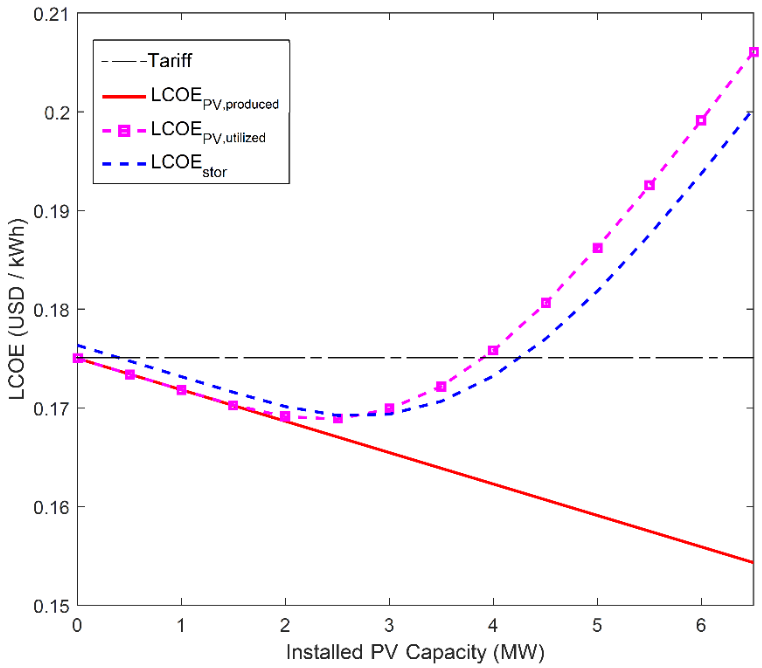

Figure 5.3. LCOE for the REMG with 0.3 MWh ZBB and 2.5 MWh PHS for different PV capacities.

The average daily values for the demand, utilized electricity generated by only PV and electricity generated by PV with ESS for configuration 3 are shown in Figure 5.4. As it is shown in the figure, average daily demand is the lowest in April, the highest in September and relatively high in July. Furthermore, the average daily discharged electricity from ZBB and PHS for each month is shown in Figure 5.5. The maximum utilized energy from ESS occurs in April which is due to the mismatch between PV system electricity generation and the demand that allows more electricity to be stored in the ESS. On the other hand, in July and September, almost no electricity from ESS is utilized since the demand is high and there is no effective possibility for charging the ESS.

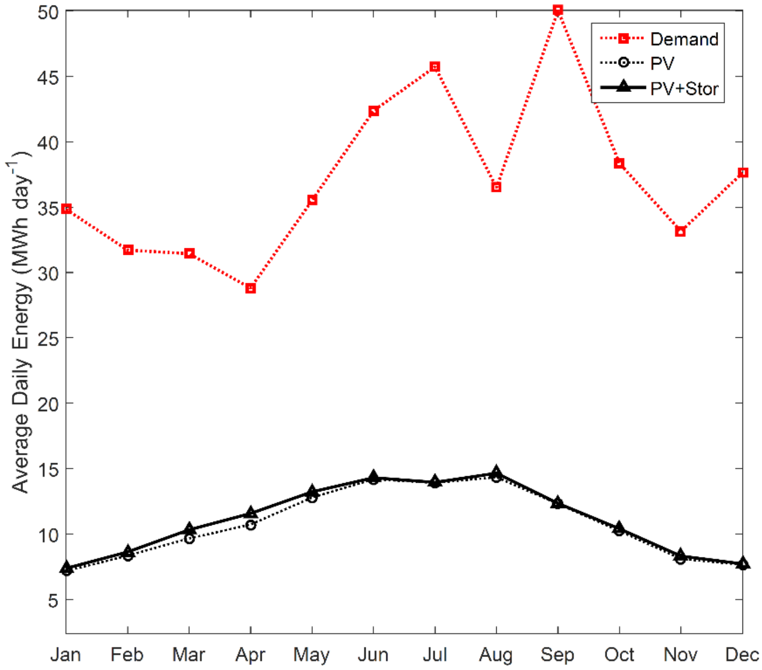

Figure 5.4. Average daily energy output for a REMG with configuration 3 and average daily demand for METU NCC for each month.

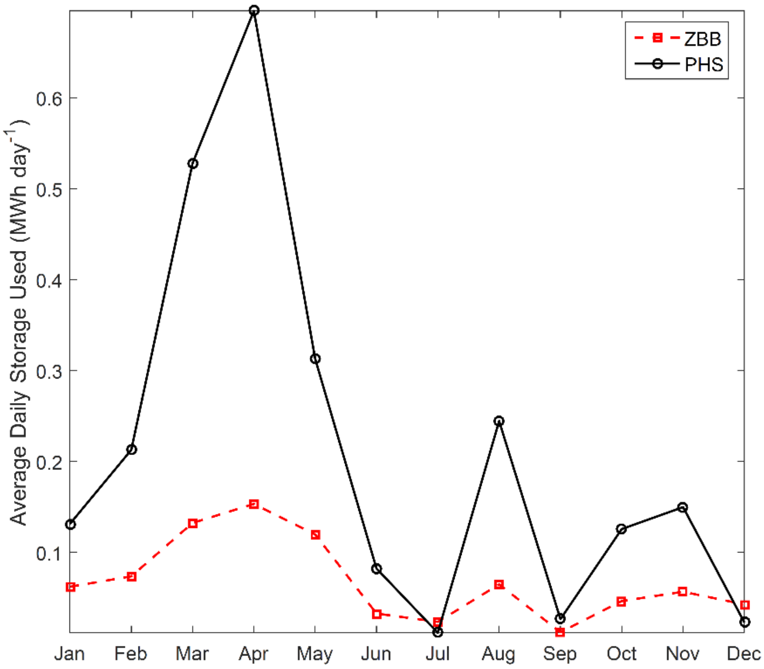

Figure 5.5. Average daily energy discharged from both ZBB (0.3 MWh) and PHS (2.5 MWh) for each month for a REMG with configuration 3.

The results show that deploying REMGs with certain configurations would be economically beneficial to meet up to 45% of the electricity demand by RES and a RES fraction of 100% would not be economically feasible yet. The requirements for a 100% RES fraction should be investigated by studying more diverse RES components, like wind, geothermal and wave energy technologies for the design of the REMG.

5.3 Case 2: Hybrid REMG Consisting PV-Wind-Battery

5.3.1 Results for the Design Conditions

The simulations are performed in HOMER considering the REMG design shown in Figure 3.3 with the potential for grid-connection in order to find the configurations with the lowest NPC. The possible installed capacities for PV, wind turbines and batteries are limited as follows: the PV system capacity is limited to a range from 0 to 5000 kW with 100 kW increment; the number of wind turbines is limited from 0 to 10 in whole numbers; and the number of batteries in the battery bank is limited from 0 to 5 units in whole numbers, each unit having 1000 kWh capacity. All designs provided by HOMER are for a grid-connected REMG, and the two designs with the lowest and almost identical NPC have similar RES fraction but fairly significant differences in architecture as shown in Table 5.4. These two designs are referred as preferred systems and considered for detailed consideration herein. All the other possible configurations in the capacity ranges defined above have higher NPC and lower RES fraction than the aforementioned two preferred configurations. Recall that the NPC includes both the REMG costs and the grid electricity costs. The REMG cost is higher for the second configuration than the first one, and this difference is almost perfectly offset by lower grid electricity costs for the second configuration relative to the first. This results in the NPC for both configurations being very close. As shown in Table 5.4, the suggested inverter capacity is lower than the suggested PV capacity in both configurations which shows that if the PV system operates at its full capacity at any time of the year, there would be excess energy which should be dumped or stored before passing through the inverter since the inverter capacity is not sufficient to utilize it. However, the analyses indicate that for 96% of the hours in the year the actual PV output is less than the inverter capacity for both configurations which indicates that the inverter capacity is sized properly. The amount of dumped electricity is 36 MWh/year corresponding to 1.0% of the total DC electricity production from the PV system for configuration 1, and 22 MWh/year corresponding to 0.6% of the total DC electricity production from the PV system for configuration 2. Note that although configuration 2 has a smaller inverter capacity, the dumped electricity for configuration 2 is also less due to the possibility of storing it using the battery. The results show that the suggested grid-connected REMG can independently supply the electricity demand of METU NCC as a standalone REMG for 1110 and 1304 hours in a year for configurations 1 and 2, respectively, which correspond to about 13% and 15% of the time in a year, respectively. The ability to island from the grid for a significant fraction of the year indicates that the designed systems for both configurations can be considered as a REMG, although in reality the connection to the grid may be required to stabilize the micro-grid under conditions of rapidly changing supply and demand. As an alternative to the grid connection, energy storage systems with relatively small capacities for short term storage purposes can be utilized to eliminate these fluctuations and enable the system to be used as REMG which should be studied as future work.

Table 5.4. System architecture for the preferred REMG for lifetime of 25 years.

Component	**Configuration 1**	**Configuration 2**
PV	2,000 kW	2,000 kW
Wind Turbine	3,000 kW	3,750 kW
Inverter	1,400 kW	1,300 kW
Battery	-	1,000 kWh
Capital Cost	9,144,800 USD	9,916,000 USD
Net Present Cost	38,014,856 USD	38,034,352 USD
LCOE	0.150 USD/kWh	0.148 USD/kWh
RES Fraction	36%	38%

The energy output as AC electricity from each component of the suggested REMG and the average daily electricity demand for each month are shown in Figure 5.6 and Figure 5.7 for configurations 1 and 2, respectively. The energy output from the PV system is higher than that from the wind energy system, although the installed capacity of wind turbines is higher for both configurations. As expected from the availability of solar resources, the electricity supplied by PV system is the highest in June, July and August due to larger solar resources, and in the case of configuration 2 the battery energy output is also higher for those months. The annual energy output from the battery in configuration 2 is 135 MWh which is about 3.7% of the annual demand. Moreover, 85% of the stored energy in configuration 2 is from the PV system and only 15% is from the wind energy system.

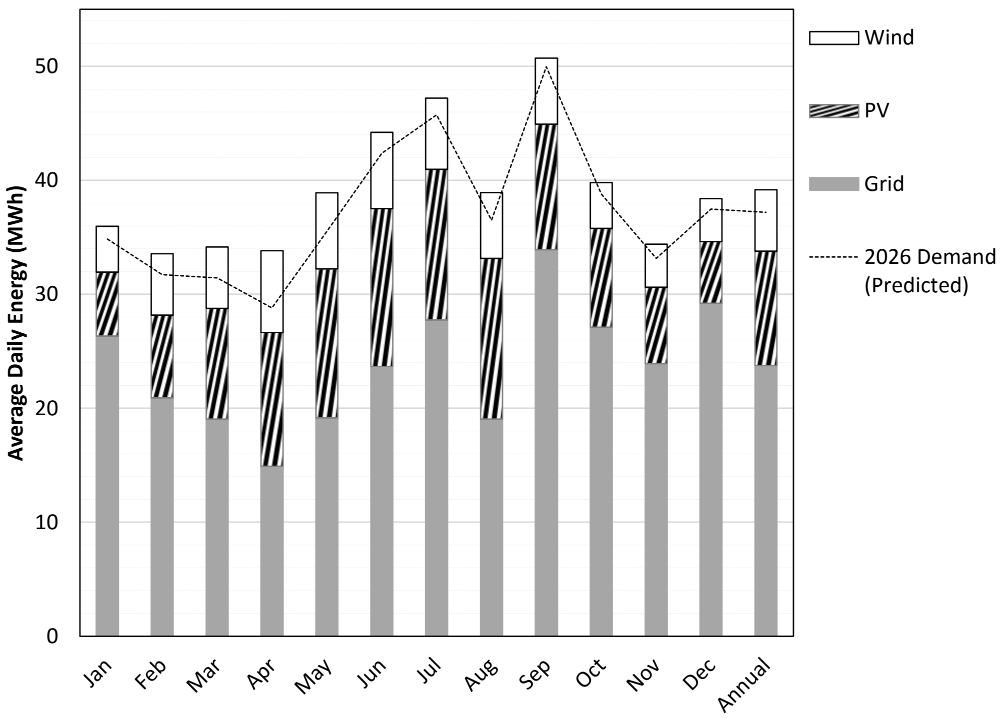

Figure 5.6. Average daily electricity demand and AC electricity production of the system components and energy supplied by the grid for configuration 1.

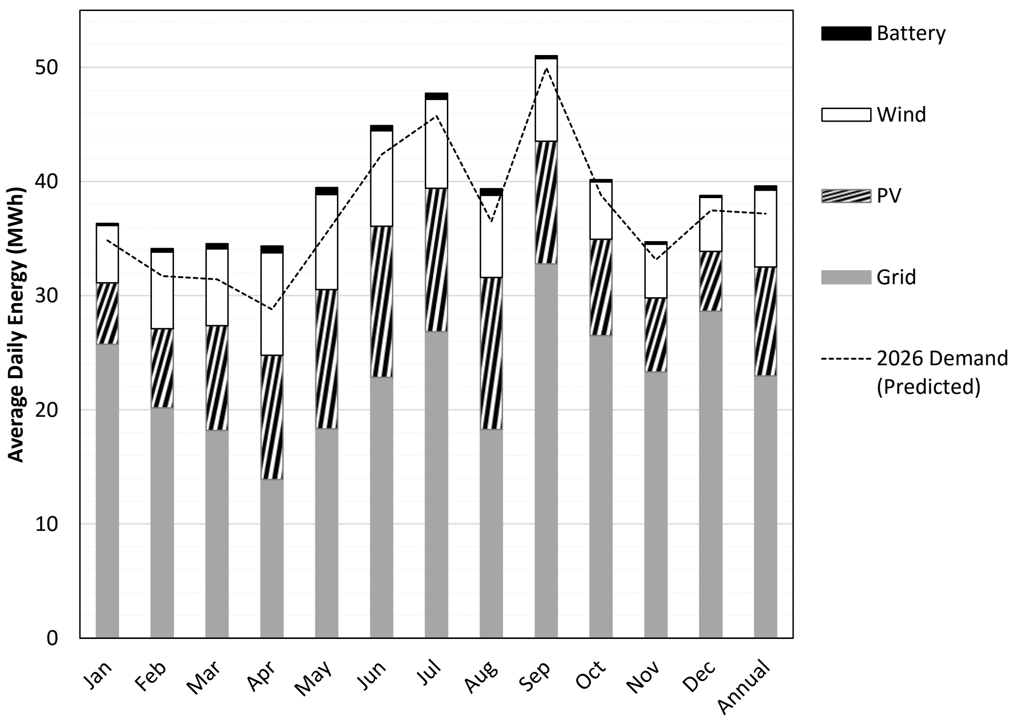

Figure 5.7. Average daily electricity demand and AC electricity production of the system components and energy supplied by the grid for configuration 2.

The solar resources are higher than wind resources at METU NCC, but the installation cost per unit capacity is less for the wind turbines than the PV system. Therefore, there should be a compromise between the PV and wind system capacities in the preferred configurations of REMG which have LCOE less than the tariff for grid electricity. In order to clarify this compromise, one should consider the cases in which RES consists of only PV system or only wind system which are given in Table 5.5, and compare them with the results for configuration 1 which consists of both PV and wind systems. This comparison shows that, having both PV and wind systems as given in configuration 1 would result in a more desirable system with lower NPC and LCOE and higher RES fraction than those of the PV only and wind only systems. Hence, the hours with large solar and wind resources tend to be different and the hours that the demand is predominately met by the PV system are different from the hours that the demand is predominately met by the wind system. Therefore, at least conceptually and at the risk of being overly simplistic, the PV and wind systems can be thought to be predominately producing electricity during different hours. Considering that solar resources are more available than wind resources at METU NCC, trying to simultaneously increase the PV capacity and decrease the wind capacity would primarily increase the donated electricity during the hours that PV output is dominant and lead to replacing wind generated electricity with grid rather than PV electricity, and ultimately lead to a higher LCOE for the REMG and lower RES fraction which are not desirable.

Table 5.5. Results for having minimum NPC if RES consists of only PV system or only wind system

RES Configuration	System Capacity for Minimum NPC (kW)	NPC (USD)	LCOE (USD/kWh)	RES Fraction (%)
PV	2300	39.6M	0.162	29
Wind Turbine	4500	39.2M	0.154	19

The average daily donated electricity for each month can be estimated for the designed REMG considering the difference between the demand and the total AC electricity generated within the REMG and supplied from the grid. The maximum donated electricity occurs in April which is due to the larger mismatch between demand, which tends to be small due to moderate temperatures, and energy production, which tends to be large due to large solar resources, compared to those for other months. As given in Table 5.4, the total RES fraction is approximately 36% and 38% for configurations 1 and 2, respectively, which excludes the electricity generated by the REMG and denoted to the grid. However, in case of having the possibility to sell the presently donated electricity to the grid by establishing two-way tariff regulations and crediting this sold electricity to the RES fraction, the RES fraction would increase to 39% and 42% for configurations 1 and 2. Generating excess electricity that is fed to the grid seems unavoidable when designing grid-connected REMG with relatively large RES fractions for small communities which is because of the large daily and seasonal variations in the demand. Two-way tariff regulations will increase the economic feasibility of grid-connected REMGs with large RES fraction and should be investigated in future studies.

Table 5.6 and Table 5.7 contain NPC for each component of the system for configurations 1 and 2, respectively. For the studied REMG, the only components which would have a fraction of their lifetime left at the end of the REMG lifetime are the inverter for configuration 1 and the battery and inverter for configuration 2. The salvage values considered for these components are given in Table 5.6 and Table 5.7. The electricity purchased from the grid has the highest share in net present cost. This higher cost gets more significant when considering recent changes in exchange rates. Because of a changing exchange rate between the local currency (Turkish Lira) and USD, the electricity tariff for METU NCC was about 0.24 USD/kWh in November 2014, while an electricity cost of 0.175 USD/kWh is considered as the current tariff. Moreover, if the demand was met by the grid only, NPC would be about 42.2M USD for 25 years which indicates 4.2M USD saving in NPC by establishing a REMG at METU NCC.

Table 5.6. Breakdown of Net Present Cost of the grid-connected REMG with configuration 1 (All costs are in USD).

Component	Capital Cost	Replacement Cost	O&M and Annual Cost	Salvage	Total Component Cost	Percentage of NPC (%)
PV	6,000,000	0	1,064,836	0	7,064,836	18%
Wind Turbine	2,164,800	0	384,193	0	2,548,993	7%
Grid	0	0	26,938,832	0	26,938,832	71%
Inverter	980,000	644,788	0	(162,588)	1,462,200	4%
System	9,144,800	644,788	28,387,864	(162,588)	38,014,856	100%

Table 5.7. Breakdown of Net Present Cost of the grid-connected REMG with configuration 2 (All costs are in USD).

Component	Capital Cost	Replacement Cost	O&M and Annual Cost	Salvage	Total Component Cost	Percentage of NPC (%)
PV	6,000,000	0	1,064,836	0	7,064,836	19%
Wind Turbine	2,706,000	0	480,241	0	3,186,241	8%
Grid	0	0	26,048,080	0	26,048,080	68%
Battery	300,000	171,676	17,747	(111,987)	377,436	1%
Inverter	910,000	598,732	0	(150,975)	1,357,757	4%
System	9,916,000	770,408	27,610,904	(262,962)	38,034,352	100%

Apart from the economic benefits of deploying REMG for METU NCC, the environmental aspects of moving towards higher fraction of RES should also be considered. Since fuel oil No. 6 is used for generating energy for the electrical grid of the island, in case of deploying the REMG given in Table 5.4 which supplies 36% to 38% of the electrical demand of METU NCC, about 4000 tons of CO_2 emissions will be avoided each year. This number is calculated using the method introduced by Tester [2] assuming 40% efficiency for steam generators and 45% efficiency for diesel generators installed on the island [73]. The amount of electricity generated is assumed to be equal for the diesel and steam generators which results in an overall efficiency of approximately 43%. It should also be noted that deploying REMG systems not only has economic benefits for the campus, but also serves educational purposes by providing laboratories on RES and connections with the industries while increasing the social awareness on the necessity of replacing conventional fossil fuels with renewable energy.

5.3.2 RES Performance Using Measured Solar and Wind Data

In this study, a grid-connected REMG for METU NCC is designed using TMY data for solar and wind resources; however, measured data are also available for this case study and the REMG performance is examined using these measured data and the results are as follows.

To examine the performance of the REMG with different availability of solar resources, *Large Measured GHI* and *Small Measured GHI* data sets are used as the inputs for the designed system, while all other inputs are the same as the design condition. The corresponding results for LCOE, NPC and RES fraction are given in Table 5.8 and Table 5.9, respectively. Compared to the design condition in which *TMY GHI* data set is used, using the *Large Measured GHI* data set as the input to the system would decrease the LCOE and NPC for both configurations. The increase in RES fraction for configuration 2 is higher since there is more energy available from PV systems that is stored in the battery. On the other hand, in case of having the *Small Measured GHI* data set as the solar resource input, the RES fraction of the suggested design configurations would decrease for both configurations.

Table 5.8. LCOE, NPC and RES fraction of the configuration 1 for *TMY GHI*, *Large Measured GHI* and *Small Measured GHI* data sets.

GHI Type	**LCOE (USD/kWh)**	**Change in LCOE (%)**	**NPC (USD)**	**Change in NPC (%)**	**RES fraction (%)**
TMY	0.150	-	38.0M	-	36
Large Measured	0.146	-3	37.1M	-2	38
Small Measured	0.160	7	40.3M	6	31

Table 5.9. LCOE, NPC and RES fraction of the system of configuration 2 for *TMY GHI*, *Large Measured GHI* and *Small Measured GHI* data sets.

GHI Type	**LCOE (USD/kWh)**	**Change in LCOE (%)**	**NPC (USD)**	**Change in NPC (%)**	**RES fraction (%)**
TMY	0.148	-	38.0M	-	36
Large Measured	0.147	-1	37.7M	-1	42
Small Measured	0.158	7	40.1M	6	34

In terms of the economic characteristics, the results given in Table 5.8 and Table 5.9 show that both configurations are robust since the resulting LCOE, NPC and RES fraction are relatively insensitive to the inputted solar resources which is an important characteristic for the system considering the variability of resources at the studied location and potential errors and uncertainties in the synthetic TMY and measured data sets.

Similarly, the measured wind data sets defined as *2014 Measured Wind* and *2015 Measured Wind* are used to analyze how the predicted performance of the designed REMG varies with variations in the inputted wind resource data. The results are given in Table 5.10 and Table 5.11 for configurations 1 and 2, respectively. The annual average wind speed in *2014 Measured Wind* and *2015 Measured Wind* data sets are greater than the one in *TMY Wind* data set, and the resulting NPC and LCOE with the measured wind data sets are significantly less and the RES fraction is 18 to 24% greater than the results with *TMY Wind* data set.

Table 5.10. LCOE, NPC and RES fraction of the system of configuration 1 for wind speed measured in 2014 and 2015.

Wind Speed Type	LCOE (USD/kWh)	Change in LCOE (%)	NPC (USD)	Change in NPC (%)	RES fraction (%)
TMY	0.150	-	38.0M	-	36
Measured 2014	0.115	-23	32.0M	-16	54
Measured 2015	0.114	-24	31.9M	-16	54

Table 5.11. LCOE, NPC and RES fraction of the system of configuration 2 for wind speed measured in 2014 and 2015.

Wind Speed Type	LCOE (USD/kWh)	Change in LCOE (%)	NPC (USD)	Change in NPC (%)	RES fraction (%)
TMY	0.148	-	38.0M	-	36
Measured 2014	0.108	-27	31.1M	-18	59
Measured 2015	0.107	-28	31.0M	-18	60

The change in LCOE, NPC and RES fraction due to utilizing measured wind speed data sets as the inputs is greater than the change due to utilizing the measured solar resources. This is because of the higher difference between measured and TMY data for wind speed, which is probably due to the higher uncertainties involved in estimating the wind resources using synthetic TMY data. Wind speed is highly dependent on microclimatic differences due to the local changes in the land/water-body characteristics including the surface roughness and altitude [71]. The measured wind speed at METU NCC were taken in an area with relatively higher altitude where the wind resources are expected to be larger than the average wind resources of the surrounding area. The solar resources are expected to be more uniform over this region than wind resources, and therefore easier to predict using Meteonorm.

5.3.3 Sensitivity of Results to Changes in Inputted Solar and Wind Resources

For further investigation of the effects of variability of solar and wind renewable energy, a sensitivity analysis is performed on solar and wind resources to investigate the effects of change in these resources on the economic performance of the system. The sensitivity study is performed by increasing or decreasing the hourly GHI and wind speed values given by *TMY GHI* proportionally to all the hours in a year. The hourly GHI and wind speed values are considered to be 80%, 90%, 110% and 120% of the hourly GHI and wind speed for TMY data. In Table 5.12 and Table 5.13, the sensitivity of NPC, LCOE and RES fraction to hourly GHI and wind speed are presented, respectively. Comparing the values given in the Table 5.12 and Table 5.13 shows that the sensitivity to increase in GHI is lower than the sensitivity to decrease in GHI which can be explained by the limited capacity of the inverter to invert more DC to AC electricity and of the battery to store the available surplus electricity for storage. The results of the sensitivity analysis show that the effects of the uncertainties in a range of ±20% in the availability of solar and wind resources are likely to result in less than ±7% change in LCOE, NPC and RES fraction.

Table 5.12. The sensitivity of LCOE, NPC and RES fraction to hourly GHI value.

Hourly GHI Configuration 1	**LCOE (USD/kWh)**	**Change in LCOE (%)**	**NPC (USD)**	**Change in NPC (%)**	**RES fraction (%)**
0.8xTMY	0.162	8	40.5M	7	30
0.9xTMY	0.156	4	39.2M	3	33
TMY	0.150	-	38.0M	-	36
1.1xTMY	0.145	-3	37.1M	-2	39
1.2xTMY	0.142	-5	36.5M	-4	41
Configuration 2					
0.8xTMY	0.160	8	40.5M	7	33
0.9xTMY	0.154	4	39.2M	3	36
TMY	0.148	-	38.0M	-	38
1.1xTMY	0.144	-3	37.2M	-2	41
1.2xTMY	0.141	-5	36.6M	-4	43

Table 5.13. The sensitivity of LCOE, NPC and RES fraction to hourly wind speed.

Hourly Wind Speed Configuration 1	**LCOE (USD/kWh)**	**Change in LCOE (%)**	**NPC (USD)**	**Change in NPC (%)**	**RES fraction (%)**
0.8xTMY	0.161	7	39.8M	5	31
0.9xTMY	0.155	3	39.0M	3	33
TMY	0.150	-	38.0M	-	36
1.1xTMY	0.144	-4	37.1M	-2	39
1.2xTMY	0.138	-8	36.1M	-5	42
Configuration 2					
0.8xTMY	0.162	9	40.1M	6	31
0.9xTMY	0.155	5	39.1M	3	33
TMY	0.148	-	38.0M	-	36
1.1xTMY	0.141	-5	36.9M	-3	39
1.2xTMY	0.134	-9	35.9M	-6	42

CHAPTER 6 – CONCLUSIONS AND FUTURE WORK

6.1 Conclusions

To investigate the feasibility of deploying renewable energy based micro-grids including PV, short-term ESS and long-term ESS for small communities, the models for each component are presented and the methodology is applied to METU NCC as a case study for small communities. ZBB and PHS are introduced as the short- and long-term ESS types, respectively. Hourly synthetic TMY data are used for estimating the available solar resources and hourly measured demand data for METU NCC are used to estimate the available energy generated by the REMG for energy storage. Based on the results, a system with no ZBB and 5.5 MWh PHS is found to have the lowest NPC; however, since having higher possibilities of islanding from the grid is desired a short-term storage to cover the delay in the starting process of the long-term ESS is considered. Moreover, the amount of available water at METU NCC only allows a maximum size of 2.5 MWh for PHS. Therefore, considering these limitations, a configuration with 2.7 MW PV, 0.3 MWh ZBB and 2.5 MWh PHS is suggested as the preferred configuration. The resulting LCOE and RES fraction are approximately 0.145 USD/kWh and 32.5%, respectively. The comparison between the NPC of different REMG configurations and NPC of providing the entire electricity demand by the grid, shows that it is economically beneficial to deploy REMG.

Moreover, the feasibility of supplying the electricity demand for remote communities by renewable energy resources is analyzed by designing a hybrid grid-connected PV-wind-battery system for a rural and isolated university community on an island with an unstable grid. A synthetic TMY data are used for the solar and wind resource data sets, while actual electricity demand data are used for the demand model.

Several configurations are simulated within the specified capacity ranges for each system component in HOMER. Based on the results, two configurations are preferred as these two have the lowest NPC among all the options. The first configuration consists of 2 MW PV and 4 wind turbines each with 750 kW rated power each (3 MW wind power in total) with no batteries yielding a NPC of 38M USD and a LCOE of 0.150 USD/kWh. The second configuration consists of 2 MW PV and 5 wind turbines each with 750 kW rated power each (3.75 MW wind power in total) with a 1 MWh battery yielding an identical NPC of 38M USD and a negligibly smaller LCOE than the one for configuration 1. The LCOE for both configurations is about 15% lower than the electricity tariff for METU NCC in 2015. Establishing a hybrid REMG would save 4M USD in NPC of supplying the electricity demand of METU NCC for 25 years. Deploying the suggested hybrid REMG would supply 36% to 38% of the METU NCC annual electrical demand which results in avoiding approximately 4000 tons of CO_2 emissions per year. The variations in the predicted performance of the designed hybrid REMG, is studied using the introduced measured data sets for solar and wind resources. Moreover, REMG's sensitivity to the availability of the solar and wind resources on the studied economic parameters are investigated. The resulting values of NPC, LCOE and RES fractions for these analyses show that the sensitivity of the system to variations in both solar and wind resources is almost at the same level, and these variations in economic performance sufficiently small that the design can be considered robust considering uncertainties in the resource models. The sensitivity of NPC for the cases with 20% lower and higher availability of solar and wind resources comparing to the design conditions resides in the range of ±7%.

6.2 Future Research Directions

The feasibility of having higher RES fraction should be investigated as a future study considering more economical storage options and through load shedding, shifting and management methodologies as part of a smart micro-grid which can function autonomously. One of the options that should be studied is the possibility of recharging the short-term ESS by the energy available in long-term ESS. This would result in having a short-term ESS for a longer time to cover the instantaneous energy needs of the REMG. Moreover, the conditions and possibility of having excess energy sale to the grid should be studied, although there is no regulation for two-way tariff in N. Cyprus yet. In addition, a 100% RES fraction would not be feasible by only PV systems and ESS, and as the future study more diverse RES should be included in the REMG configuration.

REFERENCES

[1] H. Müller-Steinhagen and F. Trieb, "Concentrating solar power," *A review of the technology. Ingenia Inform QR Acad Eng*, vol. 18, Stuttgart, Germany, pp. 43–50, 2004.

[2] J. W. Tester, *Sustainable energy: choosing among options*. MIT Press, 2005.

[3] International Energy Agency (IEA), "Technology Roadmap: Concentrating Solar Power," OECD Publishing, May 2010.

[4] S. Nagl, M. Fürsch, C. Jägemann, and M. O. Bettzüge, "The economic value of storage in renewable power systems - the case of thermal energy storage in concentrating solar plants," 2011.

[5] A. Evans, V. Strezov, and T. J. Evans, "Assessment of sustainability indicators for renewable energy technologies," *Renew. Sustain. Energy Rev.*, vol. 13, no. 5, pp. 1082–1088, 2009.

[6] F. R. Pazheri, M. F. Othman, and N. H. Malik, "A review on global renewable electricity scenario," *Renew. Sustain. Energy Rev.*, vol. 31, pp. 835–845, 2014.

[7] "Worl Bank Indicators," 2016. [Online]. Available: http://data.worldbank.org/indicator/. [Accessed: 17-Jun-2016].

[8] J. Paska, P. Biczel, and M. Kłos, "Hybrid power systems – An effective way of utilising primary energy sources," *Renew. Energy*, vol. 34, no. 11, pp. 2414–2421, Nov. 2009.

[9] T. Ma, H. Yang, and L. Lu, "A feasibility study of a stand-alone hybrid solar-wind-battery system for a remote island," *Appl. Energy*, vol. 121, pp. 149–158,

2014.

[10] C. Koroneos, M. Michailidis, and N. Moussiopoulos, “Multi-objective optimization in energy systems: The case study of Lesvos Island, Greece,” *Renew. Sustain. Energy Rev.*, vol. 8, no. 1, pp. 91–100, 2004.

[11] E. D. Giannoulis and D. a. Haralambopoulos, “Distributed generation in an isolated grid: Methodology of case study for Lesvos - Greece,” *Appl. Energy*, vol. 88, no. 7, pp. 2530–2540, 2011.

[12] a. B. Kanase-Patil, R. P. Saini, and M. P. Sharma, “Integrated renewable energy systems for off grid rural electrification of remote area,” *Renew. Energy*, vol. 35, no. 6, pp. 1342–1349, 2010.

[13] F. S. Barnes and J. Levine G., Eds., *Large energy storage systems handbook*. CRC Press, 2011.

[14] J. K. Kaldellis, Ed., *Stand-alone and hybrid wind energy systems: technology, energy storage and applications*. Elsevier, 2010.

[15] M. C. Lott and S.-I. Kim, “Technology Roadmap, Energy storage,” International Energy Agency (IEA), France, 2014.

[16] S. M. Hasnain, “Review on sustainable thermal energy storage technologies, Part II: cool thermal storage,” *Energy Convers. Manag.*, vol. 39, no. 11, pp. 1139–1153, Aug. 1998.

[17] S. M. S. Sadati, F. U. Qureshi, and D. Baker, “Energetic and economic performance analyses of photovoltaic, parabolic trough collector and wind energy systems for Multan, Pakistan,” *Renew. Sustain. Energy Rev.*, vol. 47,

pp. 844–855, 2015.

[18] A. M. Vassallo, “Applications of batteries for grid-scale energy storage,” in *Advances in Batteries for Medium and Large-Scale Energy Storage*, Woodhead Publishing Ltd, 2015, pp. 587–607.

[19] Lazard, “Lazard’s levelized cost of storage analysis — version 1.0,” *Lazard*, no. November, 2015.

[20] Primus Power, “Energy Pod,” 2015. [Online]. Available: http://www.primuspower.com/products/. [Accessed: 20-May-2016].

[21] J. K. Kaldellis, D. Zafirakis, E. L. Kaldelli, and K. Kavadias, “Cost benefit analysis of a photovoltaic-energy storage electrification solution for remote islands,” *Renew. Energy*, vol. 34, no. 5, pp. 1299–1311, 2009.

[22] M. Kintner-Meyer, M. Elizondo, P. Balducci, C. Jin, T. Nguyen, F. Tuffner, and X. Guo, *Energy Storage for Power Systems Applications: A Regional Assessment for the Northwest Power Pool (NWPP)*, no. April. US Department of Energy, 2010.

[23] S. M. S. Sadati, E. Jahani, O. Taylan, and D. K. Baker, “Feasibility Study of a Renewable Energy Micro-Grid for a Mediterranean Island Community,” Submitted, 2016.

[24] P. Denholm and M. Hand, “Grid flexibility and storage required to achieve very high penetration of variable renewable electricity,” *Energy Policy*, vol. 39, no. 3, pp. 1817–1830, 2011.

[25] J. K. Kaldellis, D. Zafirakis, and E. Kondili, “Optimum sizing of photovoltaic-

energy storage systems for autonomous small islands," *Int. J. Electr. Power Energy Syst.*, vol. 32, no. 1, pp. 24–36, 2010.

[26] C. Harris, J. P. Meyers, and M. E. Webber, "A unit commitment study of the application of energy storage toward the integration of renewable generation," *J. Renew. Sustain. Energy*, vol. 4, no. 1, p. 13120, 2012.

[27] A. Gil, M. Medrano, I. Martorell, A. Lázaro, P. Dolado, B. Zalba, and L. F. Cabeza, "State of the art on high temperature thermal energy storage for power generation. Part 1—Concepts, materials and modellization," *Renew. Sustain. Energy Rev.*, vol. 14, no. 1, pp. 31–55, 2010.

[28] C. Gatzen, *The economics of power storage: theory and empirical analysis for central europe*. Oldenbourg Industrieverlag, 2008.

[29] P. Denholm, E. Ela, B. Kirby, and M. Milligan, "The role of energy storage with renewable electricity generation," pp. 1–61, 2010.

[30] P. Denholm, J. Jorgenson, T. Jenkin, D. Palchak, B. Kirby, and M. O. Malley, "The value of energy storage for grid applications," no. May, p. 37, 2013.

[31] M. Carbajales-Dale, C. J. Barnhart, and S. M. Benson, "Can we afford storage? A dynamic net energy analysis of renewable electricity generation supported by energy storage," *Energy Environ. Sci.*, vol. 7, p. 1538, 2014.

[32] A. Andrijanovits, H. Hoimoja, and D. Vinnikov, "Comparative Review of Long-Term Energy Storage Technologies for Renewable Energy Systems," *Electron. Electr. Eng.*, vol. 118, no. 2, Feb. 2012.

[33] F. Jos, "Optimization of hybrid renewable energy systems," University of

Toronto, 2015.

[34] J. Kathan, J. Von Appen, E. Rikos, L. Grigans, L. Atte, E. Micolano, and D. Burnier de Castro, “Report: EERA Joint Programme Deliverable,” European Energy Research Alliance, 2014.

[35] L. Tao, L. Mo, S. Liu, and R. X. Gao, “Optimal Battery Charge and Discharge Control Scheme Under Solar Power Inflow,” in *2012 IEEE I2MTC - International Instrumentation and Measurement Technology Conference, Proceedings*, 2012, no. 1, pp. 849–854.

[36] L. Xu, X. Ruan, C. Mao, B. Zhang, and Y. Luo, “An Improved Optimal Sizing Method for Wind-Solar-Battery Hybrid Power System,” *IEEE Trans. Sustain. Energy*, vol. 4, no. 3, pp. 774–785, 2013.

[37] S. M. H. Ali, M. J. S. Zuberi, M. A. Tariq, D. Baker, and A. Mohiuddin, “A study to incorporate renewable energy technologies into the power portfolio of Karachi, Pakistan,” *Renew. Sustain. Energy Rev.*, vol. 47, pp. 14–22, Jul. 2015.

[38] S. Chakrabarti and S. Chakrabarti, “Rural electrification programme with solar energy in remote region–a case study in an island,” *Energy Policy*, vol. 30, no. 1, pp. 33–42, Jan. 2002.

[39] A. Asrari, A. Ghasemi, and M. H. Javidi, “Economic evaluation of hybrid renewable energy systems for rural electrification in Iran - A case study,” *Renew. Sustain. Energy Rev.*, vol. 16, no. 5, pp. 3123–3130, 2012.

[40] I. B. Askari and M. Ameri, “Techno-economic feasibility analysis of stand-alone renewable energy systems (PV/bat, wind/bat and hybrid PV/wind/bat) in Kerman, Iran,” *Energy Sources, Part B Econ. Planning, Policy*, vol. 7, no. May

2015, pp. 45–60, 2012.

[41] G. Bekele and B. Palm, “Feasibility study for a standalone solar-wind-based hybrid energy system for application in Ethiopia,” *Appl. Energy*, vol. 87, no. 2, pp. 487–495, 2010.

[42] G. Bekele and G. Tadesse, “Feasibility study of small Hydro/PV/Wind hybrid system for off-grid rural electrification in Ethiopia,” *Appl. Energy*, vol. 97, pp. 5–15, 2012.

[43] A. H. Al-Badi, M. H. Albadi, A. Malik, M. Al-Hilali, A. Al-Busaidi, and S. Al-Omairi, “Levellised electricity cost for wind and PV–diesel hybrid system in Oman at selected sites,” *Int. J. Sustain. Eng.*, no. May 2015, pp. 37–41, 2013.

[44] The HOMER Energy Team, “The HOMER® Microgrid Software.” 2015.

[45] WeatherOnline Ltd., “Oman Climate,” 2015. [Online]. Available: http://www.weatheronline.co.uk/reports/climate/Oman.htm. [Accessed: 20-Sep-2015].

[46] Hong Kong Government, “Climate of Hong Kong.” [Online]. Available: http://www.hko.gov.hk/cis/climahk_e.htm. [Accessed: 20-Sep-2015].

[47] W. P. M. R. Pathirana and A. Muhtaroğlu, “Multifaceted feasibility analysis of pv solar application in northern cyprus,” vol. 3, no. 4, 2013.

[48] M. A. Tariq, “Methodology to size large scale solar pv installations for institutions with unidirectional metering,” Middle East Technical University, Northern Cyprus Campus, 2014.

[49] Meteotest Co., “Meteonorm Software,” 2015. [Online]. Available:

http://meteonorm.com/. [Accessed: 27-Apr-2015].

[50] M. Yenen, “Modeling electrical energy production in northwestern cyprus based on solar and wind measurements,” Middle East Technical University, Northern Cyprus Campus, 2015.

[51] S. M. S. Sadati, E. Jahani, and O. Taylan, “Technical and economic analyses for sizing PV power plant with storage system for METU NCC,” in *ASME 2015 International Mechanical Engineering Congress and Exposition*, 2015, pp. V06BT07A044–V06BT07A044.

[52] M. Kapsali, J. S. Anagnostopoulos, and J. K. Kaldellis, “Wind powered pumped-hydro storage systems for remote islands: A complete sensitivity analysis based on economic perspectives,” *Appl. Energy*, vol. 99, pp. 430–444, Nov. 2012.

[53] CanadianSolar Co., “CS6X-P Data Sheet,” 2015. [Online]. Available: http://www.canadiansolar.com/product/cs6x-p.html. [Accessed: 27-Apr-2015].

[54] N. H. Reich, B. Mueller, A. Armbruster, W. G. Sark, K. Kiefer, and C. Reise, “Performance ratio revisited: is PR> 90% realistic?,” *Prog. Photovoltaics Res. Appl.*, vol. 20, no. 6, pp. 717–726, 2012.

[55] Y. Ueda, K. Kurokawa, K. Kitamura, M. Yokota, K. Akanuma, and H. Sugihara, “Performance analysis of various system configurations on grid-connected residential PV systems,” *Sol. Energy Mater. Sol. Cells*, vol. 93, no. 6–7, pp. 945–949, 2009.

[56] J. Hernández-Moro and J. M. Martínez-Duart, “Analytical model for solar PV and CSP electricity costs: Present LCOE values and their future evolution,”

Renew. Sustain. Energy Rev., vol. 20, pp. 119–132, Apr. 2013.

[57] Ö. Muhtaroglu, "State planning organization," N. Cyprus Economic Planning Department, 2012.

[58] National Renewable Energy Laboratory (NREL), "Cost report: Cost and performance data for power generation," 2012.

[59] Wholesale Solar, "Inverter Prices," 2015. [Online]. Available: http://www.wholesalesolar.com/power-inverters. [Accessed: 03-Oct-2015].

[60] A. Maleki and F. Pourfayaz, "Sizing of stand-alone photovoltaic/wind/diesel system with battery and fuel cell storage devices by harmony search algorithm," *J. Energy Storage*, vol. 2, pp. 30–42, Aug. 2015.

[61] "Local electricity authority (Kib-Tek)." [Online]. Available: https://www.kibtek.com/. [Accessed: 09-Sep-2015].

[62] F. a. Canales and A. Beluco, "Modeling pumped hydro storage with the micropower optimization model (HOMER)," *J. Renew. Sustain. Energy*, vol. 6, no. 4, p. 043131, 2014.

[63] T. Lambert, P. GILMAN, and P. LILIENTHAL, "Micropower system modeling with Homer," Homer Energy, 2006, p. 402.

[64] Astm, "ASTM E1049-85: Standard Practices for Cycle Counting in Fatigue Analysis," 2011.

[65] "SolarGIS," 2016. [Online]. Available: http://solargis.com/products/maps-and-gis-data. [Accessed: 18-Jun-2016].

[66] Meteotest Co., "Difference map Meteonorm version," 2015. [Online].

Available: http://meteonorm.com/en/support/faq_post/differenzkarte-version-6.1-zu-version-7. [Accessed: 17-Aug-2015].

[67] PVsyst, “Meteo data comparisons,” 2015. [Online]. Available: http://www.pvsyst.com/en/publications/meteo-data-comparaisons. [Accessed: 17-Aug-2015].

[68] K. Skeiker, “Comparison of methodologies for TMY generation using 10 years data for Damascus, Syria,” *Energy Convers. Manag.*, vol. 48, no. 7, pp. 2090–2102, Jul. 2007.

[69] J. A. Duffie and W. A. Beckman, “Solar engineering of thermal processes,” *Wiley Sons, New York, pg*, vol. 216, p. 230, 1991.

[70] D. G. Erbs, S. A. Klein, and J. A. Duffie, “Estimation of the diffuse radiation fraction for hourly, daily and monthly-average global radiation,” *Sol. energy*, vol. 28, no. 4, pp. 293–302, 1982.

[71] H. K. Johnson, “Simple expressions for correcting wind speed data for elevation,” *Coast. Eng.*, vol. 36, no. 3, pp. 263–269, Apr. 1999.

[72] S. M. H. Ali, “Optimal photovoltaic size estimation for a campus area considering uncertainties in load, power generation and electricity rates,” Middle East Technical University, 2015.

[73] L. Honorio, J.-G. Barataire, R. Bauershmidt, T. Ohman, Z. Tihanyi, H. Zeinhofer, J. F. Scowcroft, and V. De Janeiro, “Efficiency in electricity generation,” 2003.

[74] S. M. Hasnain, “Review on sustainable thermal energy storage technologies,

Part I: heat storage materials and techniques," *Energy Convers. Manag.*, vol. 39, no. 11, pp. 1127–1138, Aug. 1998.

[75] B. Zalba, J. M. Marín, L. F. Cabeza, and H. Mehling, "Review on thermal energy storage with phase change: materials, heat transfer analysis and applications," *Appl. Therm. Eng.*, vol. 23, no. 3, pp. 251–283, 2003.

[76] G. Beckmann and P. V. Gilli, "Thermal energy storage: Basics, design, applications to power generation and heat supply," Jan. 1984.

[77] H. Ibrahim, A. Ilinca, and J. Perron, "Energy storage systems—Characteristics and comparisons," *Renew. Sustain. Energy Rev.*, vol. 12, no. 5, pp. 1221–1250, 2008.

APPENDIX

APPENDIX A – ENERGY STORAGE TYPES AND CHARACTERISTICS

There are several types of energy storage systems (ESS) which can be utilized in different sizes which cover residential to grid scale applications. In this section, thermal, compressed air, pumped hydro and battery energy storage systems are briefly introduced. Although the batteries are introduced as the last ESS type in this section, they are more likely to be used in the case of micro-grids, mainly because they are more scalable comparing to other ESS types [18].

A.1 Thermal Energy Storage (TES) Types

Using heated materials in specific containers the extra amount of thermal energy achieved from concentrated solar power plants can be stored. There are mainly two types of heat storages: a) Sensible Heat Storage and b) Latent Heat Storage.

A.1.1 Sensible Heat Storage

It is desired to have high specific heat capacity, long term stability in the case of thermal cycling, compatibility with its containment and low cost for storage medium for sensible heat method [74]. The materials that are used for sensible heat storage might be chosen in liquid or solid form. Due to its high specific heat, water is the first candidate as a liquid. Water is an appropriate choice for low temperature storages (say ~25-90°C) [74]. For a 60°C change in temperature water will store 252 kJ/kg or 2.52×10^5 kJ/m^3 since its specific heat is 4.2 kJ/kg.

Nevertheless, some molten salts and petroleum based oils with lower specific heat are also used as the medium for heat storage in higher temperatures since they have lower vapor pressure than water. The lower vapor pressure makes it applicable to store them with higher temperatures than water vapor in the same container. Table A.1 contains the characteristics of several materials for being used as the main substance for sensible TES.

Table A.1. Comparison of various heat storage media (stored energy= 10^6 kJ=300 kWh; T =15 K) [74].

	Sensible heat storage		**Phase Change Materials**	
	Rock	**Water**	**Organic**	**Inorganic**
Latent heat of fusion (kJ/kg)	-	-	190	230
Specific heat (kJ/kg)	1.0	4.2	2.0	2.0
Density (kg/m3)	2240	1000	800	1600
Storage mass for storing 10^6 kJ (kg)	67000	16000	5300	4350
Relative mass**	15.0	4.0	1.3	1.0
Storage volume for storing 10^6 kJ (m3)	30.0	16.0	6.6	2.7
Relative volume**	11.0	6.0	2.5	1.0

*Latent heat of fusion is not of interest for sensible heat storage.

**Relative mass and volume are based on latent heat storage in inorganic phase change materials

A.1.2 Latent Heat Storage (Phase Change Materials)

Energy is stored by phase change in the material. For instance, the material may change its form from solid to liquid and this will store the amount of energy used for this process. The use of phase change materials is a more secure way to store the solar thermal energy. There are a wide range of materials investigated in a large number of studies and used for this purpose [13], [74], [75].

Melting Temperature, heat fusion and heat conductivity is given for a great number of materials in [75]. As an example Table A.2 shows the thermal properties of different materials that can be used as the storage media for latent heat.

There are two important advantages for storage of heat energy using phase change materials [74]. Firstly, high energy storage density in case of using latent storage makes it possible to store more amount of energy. For example, the energy needed to melt 1 kg of ice without raising the temperature is 80 times greater than the energy needed for raising water temperature from 0°C to 1°C. Secondly, by using phase change materials it is possible to store energy in a constant temperature.

The three components needed for latent thermal storage are: a) a substance for heat storage which undergoes solid to liquid phase change process in the desired temperature and stores the heat consumed for fusion, b) a container that holds the material and c) a heat exchanger to transfer heat from the source to the material in the container [74].

Mostly used materials for phase change heat storage are: salt hydrates, paraffins, non-paraffin organics, eutectics and some salt mixtures [74], [75]. It is important to choose the type of container in order to prevent any reaction between the material used for the container and the storage substance. This is important for safety issues and to avoid any corrosions on the container.

The heat exchanger design is an important step in the latent heat storage method. The heat exchanger will transfer the heat to the substance in the container and will also transfer the thermal energy from substance to the energy sink. The temperature gradient is important in heat exchangers in charging and discharging processes.

Table A.2. Latent heat storage materials and their temperature ranges (adapted from [74]).

Temperature Range (°C)	Material	Transition Temperature (°C)	Heat of Fusion (kJ/kg)
0-100	Water	0	335
	Paraffin	20-60	140-280
	Salt hydrate	30-50	170-270
100-400	$AlC1_3$	192	280
	$LiNO_3$	250	370
	Na_2O_2	360	314
400-800	50LiOH/50LiF	427	512
	KC_1O_4	527	1253
	LiH	699	2678
800-1500	LiF	868	932
	NaF	993	750
	MgF_2	1271	936
	Si	1415	1654

The material used for container and the whole structure undergo high temperatures and they should be designed in order to tolerate the structural excitations due to the thermal gradient. The thermal expansion of a material must be taken into account in the process of storage system design [13]. Thermal strain is calculated as:

$$\Delta x = \alpha \Delta T L \tag{A.1}$$

where Δx is elongation, α is thermal strain coefficient, ΔT is the thermal gradient and L is the initial length of the material. In the design process both mechanical and thermal stress and strain should be taken into account [76]. The relation between temperature and thermal energy for sensible and latent energy storage are schematically shown in Figure A.1.

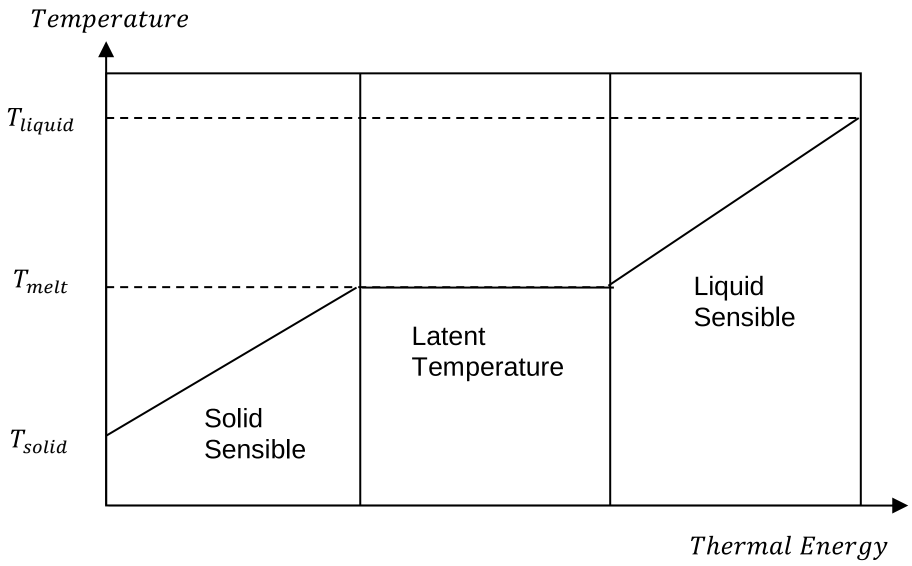

Figure A.1. Schematic plot of temperature vs thermal energy for materials undergoing phase change [13].

Energy can also be stored in other forms than thermal. The following is the other ways of energy storages used in power plants typically.

A.2 Compressed Air

It is possible to store the thermal energy converted to the compressed air. The amount of energy used for compressing the air will be achieved from the excessive electricity generated in off-peak hours.

The air will be compressed to pressures as high as 40 to 70 bars at a temperature near ambient. The higher pressure means less volume and consequently the storage reservoir will be smaller. Many studies have been done on storage of compressed air underground [77]. Figure A.2 shows three different ways of storing compressed air underground using high pressure piping.

The enrgy stored for this kind of systems is ~12 kWh/m^3 and the estimated efficiency is around 70% [77]. The energy required to store ample amount of air to produce 1 kWh electricity to be released into the network when demanded is 0.7kWh-0.8kWh. This amount of energy will be achieved during the off-peak hours.

This kind of storage system with underground storage reservoir is in operation since 1978 in Huntorf, near Bremen, Germany [77]. It is important to avoid any leakage in the reservoir or through the pipelines inorder to maximize the efficiency.

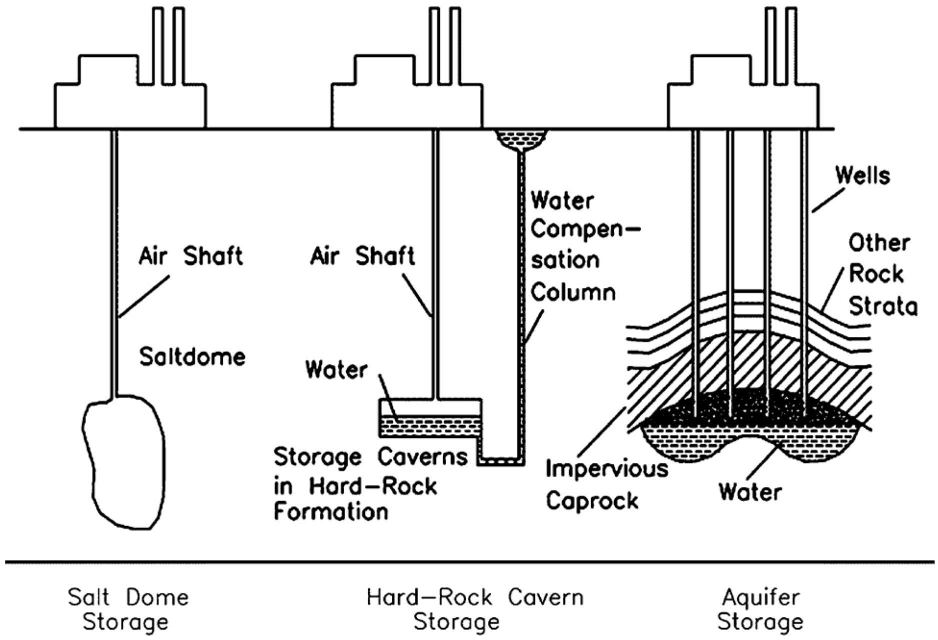

Figure A.2. Different types of compressed air storage reservoirs (copied from [77]).

A.3 Pumped Hydro Storage (PHS)

Pumped hydro energy storage system is quite convenient to install and use. For high-power applications this technology is the most used one currently [77]. The fundamental concept is similar to compressed air energy storage: during off-peak the produced electrical energy will be used to pump the water to a reservoir in a higher elevation. So the energy will be stored in water in the form of potential gravity. When the electricity is highly demanded the water in upper reservoir will be released and the electrical energy will be produced by using a turbine. The required volume of water for the given head to store 1 MWh of energy assuming 98% turbine efficiency is shown in Figure A.3.

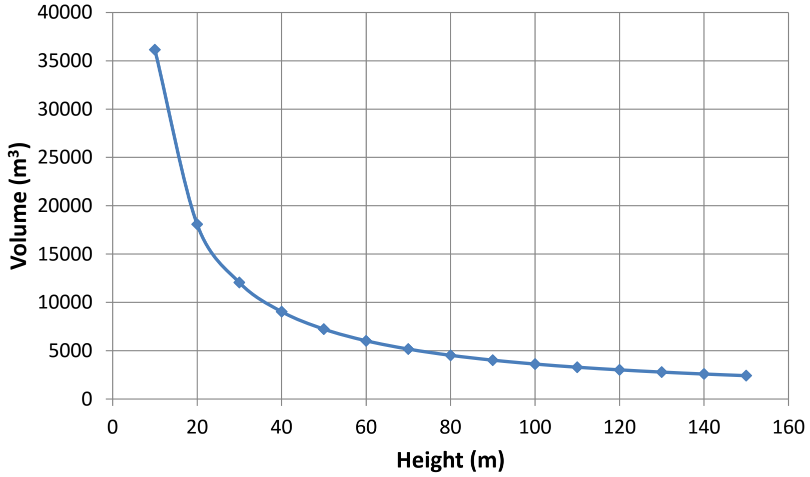

Figure A.3. Water volume needed at a given height to store 1 MWh energy with 98% turbine efficiency.

Dominion Power's Bath County pumped hydro energy storage station is an example of the introduced system which is in operation since 1985. Net generation capacity of this station is around 2100 MW. Table A.3 shows the specifications of the mentioned PHS system in more details including the total cost of the storage system installation.

Table A.3. Specifications of Dominion Power's Bath County PHS Station [13].

Net generating capacity	2100 MW
License issued	January 1977
Commercial Operation	Since December 1985
Cost (1985)	$1.7 billion ($810/MW)
Lower dam	41 m high; 671 m long; contains 3.1×10^6 m^3
Lower reservoir	2.25 km^2; water level fluctuates 18 m during the operation
Upper dam	140 m high; 671 m long; contains 13.8×10^6 m^3
Upper reservoir	1.07 km^2 water level fluctuates 32 m during the operation

The efficiency of PHS is studied in [13]. The terms that influence the efficiency are the losses as the result of resistance, turbulence and losses in the motor generator and pump turbine. So depending on design characteristics the conversion efficiency depending on the equipment characteristics is around 65-80% [13]**.** For example, 80% efficiency means that for every 10 units of energy used for pumping the water to upper reservoir, 8 units will be returned in high demand hours. Table A.4 contains the common efficiency values for components of a PHS.

Table A.4. PHS Cycling Efficiency [13].

	Low %	High %
Generating Components		
Water conductors	97.40	98.50
Pump turbine	91.50	92.00
Generator motor	98.50	99.00
Transformer	99.50	99.70
Subtotal	87.35	89.44
Pumping Components		
Water conductors	97.60	98.50
Pump turbine	91.60	92.50
Generator motor	98.70	99.00
Transformer	99.50	99.80
Subtotal	87.80	90.02
Operational	98.00	99.50
Total	75.15%	80.12%

A.4 Batteries

Electrochemical energy storage is one of the ESS types considered for both residential and grid scale energy storage applications [13], [14], [18]. Batteries are advantageous because of their scalability, quietness and high efficiency. In terms of residential applications, batteries seem to be the only available option as the ESS. There are different types of batteries having different characteristics and costs which makes them suitable for various purposes. Commonly used types are Lead-Acid batteries, Lithium-ion (LiB) batteries, Flow batteries (including Vanadium Redox), Sodium-Sulfur (NaS) batteries [13], [18]. There are also other types of batteries which are more advanced but not commonly used yet mainly because of their costs. However, there are ongoing researches on these types to make them available for residential and grid scale applications. Supercapacitors are one of these types with potential to store considerable amount of energy for grid scale applications [18]. Some characteristics of the commonly used batteries are shown in Table A.5.

Table A.5. Typical characteristics for common battery types [13].

	Lead-Acid	**NaS**	**LiB**	**Vanadium Redox**
Specific energy (Wh/kg)	10 to 35	133 to 202	150	20 to 30
Specific power (W/kg)	50 to 90	285 to 345	400	30
Cycle life	200 to 700	2500 to 4500	1000	12000